ONSET OF THE NEOGENE - QUATERNARY CONTINENTAL SOUTHERN MALAWI RIFT AND LINKAGE TO THE LATE CARBONIFEROUS – EARLY JURASSIC SHIRE RIFT

By

OYEWANDE OLUMIDE OJO

Bachelor of Science in Geology

University of Ibadan

Ibadan, Oyo State

2015

Submitted to the Faculty of the
Graduate College of the
Oklahoma State University
in partial fulfillment of
the requirements for
the Degree of
MASTER OF SCIENCE
July, 2021

ONSET OF THE NEOGENE - QUATERNARY CONTINENTAL SOUTHERN MALAWI RIFT AND LINKAGE TO THE LATE CARBONIFEROUS – EARLY JURASSIC SHIRE RIFT

Thesis Approved:

Dr. Daniel A. Laó-Dávila

Thesis Adviser

Dr. Mohamed Abdelsalam

Dr. James Knapp

ACKNOWLEDGEMENTS

I would like to thank God for the successful completion of this research. I would like to express deep appreciation to my committee chair and advisor, Dr. Daniel A. Laó Dávila, for his continued and convincing spirit of adventure regarding research. This project would not have been possible without his guidance and persistent help. I would also like to thank my committee members (Dr. Mohamed Abdelsalam and Dr. James Knapp) for their support, suggestions and feedbacks towards the successful completion of this research.

My gratitude also goes to Dr. Stuart Thomson and the Fission Track Laboratory at University of Arizona for their collaboration and hospitality while I was there in Tucson for the thermochronology measururements. I would also like to thank the NSF-funded GSA AGeS2 Program that funded this research. It was an honor to be trusted with the funds to bring our proposal to reality.

I would also like to thank my colleagues at the Boone Pickens School of Geology for their support throughout this program.

Finally, I would like to thank my parents and sisters for their love and support always. None of these would have been possible without you guys. You rock!

Name: OYEWANDE OJO

Date of Degree: JULY, 2021

Title of Study: ONSET OF THE NEOGENE - QUATERNARY CONTINENTAL SOUTHERN MALAWI RIFT AND LINKAGE TO THE LATE CARBONIFEROUS – EARLY JURASSIC SHIRE RIFT

Major Field: GEOLOGY

Abstract:

Previous thermal history models have supported Miocene aged rift initiation in northern Malawi Rift without the thermal history of southern Malawi Rift (which is believed to have initiated at a later time) and its interactions with the relic of an older rift system along the Shire Rift just south of it. New thermal history models, derived from new apatite fission-track data from this study, outline three distinct cooling episodes in the Cretaceous, Eocene–Oligocene and Miocene–Pliocene that suggest the southern Malawi Rift has been accommodating strain along their border faults since the Miocene just as the northern Malawi Rift. Our thermal modelling approach combines thermochronology and previous published geochronology with the Monte Carlo approach of the HeFTy software.

The timing and rate of rock uplift were further constrained through application of remote sensing fracture strain analyses. These results, when combined with our thermal history modeling results, yield inferred deformation strain rates that support linkage between the two rift systems. Exhumation histories show the southern Malawi Rift has likely been uplifting since the Early Miocene just as the northern Malawi Rift and its growth and evolution has caused linkage and transfer of strain between southern Malawi Rift and the older Shire Rift which appears to have been reactivated and accommodating strain since Pliocene. These results provide evidence of coeval extension across the Western Branch of the East African Rift System which has implications for the tectonic evolution of the East African Rift system.

TABLE OF CONTENTS

LIST OF TABLES

LIST OF FIGURES

Figure Page

CHAPTER I

INTRODUCTION

Continental Rifts are key features of the plate tectonics paradigm; extension accommodated along divergent boundaries through continental rifting especially at their early stages remains vital to the understanding of the dynamics of the processes and products of plate tectonics. Strain accommodation in the upper crust during continental rifting is usually manifested by formation, propagation, and linkage of normal faults and rift basins (Muirhead et al., 2019; Nixon et al., 2016, Calais et al., 2008). The way faults grow is influenced by the stress field of the fracture network, pre-existing structures, and lithospheric heterogeneities (Rotevatn et al., 2019, Peacock et al., 2017, Nixon et al., 2016). Strain accommodation and transfer control the architecture and geometry of early-stage continental rift as often observed in the active border faults and other fracture systems along the rift axes (Muirhead et al., 2019; Nixon et al., 2016). The term strain accommodation for the purpose of this study refers to the style or pattern of strain along a rift system in response to the tectonic stress acting on it.

Researchers are still unsure how continental rifts grow, propagate, and evolve, specially at early stages. Strain accommodation and transfer between rift systems is an important component of continental rift evolution. Previous studies show the evolution of faulting along continental rifts can be inferred from series of structural and tectonic attributes along the rift (Bonini et al., 2005).

These attributes include the direction of younging of the border faults (Abbate and Sagri, 1980; WoldeGabriel et al., 1990, 2016), the increase in the elastic thickness of the lithosphere and border fault length (Hayward and Ebinger, 1996), increase in delay times between the fast and slow S waves correlating with an increase in strain and with lower crustal residence times for erupted lavas (Furman et al., 2004; Maguire et al., 2003), migration of the volcanism from the region (Zanettin et al., 1980), and deepening of mantle intrusion below the rift axis and higher alkalinity of basalts (Mahatsente et al., 1999).

The linking and interaction between adjacent rift segments, as they propagate, typically occurs where structurally complex areas (e.g., transfer zones) have allowed along-axis changes in subsidence of grabens and elevation of uplifted flanks (Rosendahl, 1987; Morley et al., 1990; Faulds and Varga, 1998; Morley, 1999). Analog and experimental models reveal 5 potential types of rift linkage across basins: three types where rifts bend away from the inherited structure (connecting via a wide or narrow rift or by forming a rotating microplate), a type where rifts bend towards it, and straight rift linkage (Brune et al., 2017). Strain is concentrated in these areas of rift linkage to take up displacement variations along the faults and to accommodate space problems created by fault interaction (Bell et al., 2014).

The Malawi Rift is one of such early-stage magma-poor continental rift that trends N-S and seems to terminate to the south at the NW-SE trending Shire Graben. The Shire Graben is considered a Paleozoic-Mesozoic rift because the sedimentary rocks in the basin are of those eras (Castaing, 1991). However, the steep scarps of the Thyolo Fault, a border fault segment of the Shire Rift and the recent earthquakes along strike (e.g., 2007 M4.8 earthquake) suggest that the rift has been reactivated and that strain from the Malawi Rift is being transferred along the Shire Graben making it difficult to be sure of how it evolves.

This brings about the problems of understanding the mechanism and model of continental rift growth. The debate of whether strain accommodation started at the same time but at different rates along the Malawi Rift or if strain accommodation started at different times and propagated along the rift continues to remain unanswered. The question of why the Northern Malawi Rift seems to have border faults that are considered to be mechanically incapable of accommodating more strain because it has reached its maximum displacement (Muirhead et al., 2016; 2019; Wedmore et al., 2020) and the Southern Malawi which have similar border faults in terms of length are still accommodating strains have brought about quite a few hypotheses over the years. The debate is based on a chronological progression in a zipper-like fashion (Vink, 1982; Specht and Rosendahl, 1989) vs coeval opening models of continental rifting (Stamp et al., 2008; 2018; 2021). The most widely accepted is the southward propagation of the Malawi Rift believed to have initiated in the northern part of the rift (Vink, 1982; Specht and Rosendahl, 1989) which suggest a zipper-like fashion of rift initiation and propagation. Another plausible explanation is a coeval Malawi Rift accommodating strain at different rates along the rift across the northern part and the southern part of the rift with respect to the location of the Euler pole of rotation for the two divergent plates (Nubian and Rovuma plates; Saria et al., 2013; Stamp et al., 2021).

Although there are some known ages for the onset of rifting from studies along the Livingstone Fault in northern Malawi Rift (Van der Beek et al., 1998; Mortimer et al., 2016), and of cooling of the Chilwa Alkaline Province in southern Malawi (Eby et al., 1995), there remains a knowledge gap in geochronological data to constrain ages of onset of strain accommodation and transfer in southern Malawi and Shire Graben. Moreover, there is a lack of imaging of upper crustal structures in the transfer zone of these two rifts. Thus, we do not know how strain is being accommodated when these two rift basins with different tectonic histories and orientations link.

This research focuses on the region in the southern part of the Malawi Rift and the northern part of the Shire Rift and intends to answer the following questions: 1.) when did

Cenozoic Rifting begin in the southern Malawi Rift? and 2.) is there Cenozoic rifting in the Shire Rift? We hypothesize that: 1) The initiation of rifting in the southern Malawi Rift is relatively younger than the northern Malawi Rift (Castaing et al., 1991; Daszinnies et al., 2008) 2) The geometry of the Southern Malawi Rift and Palaeozoic-Mesozoic Shire Rift at the transfer zone indicates strain is being accommodated by rift linkage of isolated and distributed faults; hence there are evidence of Cenozoic rifting in the Shire Rift.

This study is designed to provide new data benefitting from previously collected data from Paleozoic-Mesozoic Shire Graben (Castaing, 1991), the Cretaceous Chilwa Alkaline Province (Eby et al., 1995), and the northern Malawi Rift (Van der Beek et al., 1998; Mortimer et al., 2016). Using the Malawi rift as a case study, we intend to contribute to the longstanding question of how strain is accommodated and transferred along rifts over time. The cooling ages of footwall rocks resulting from this study will provide important basis for comparison of the strain accommodation (Thomson et al., 1998; Raab et al., 2002, 2005) along the Malawi Rift and the Shire Graben.

Strain accommodation along rift systems is often accompanied by uplift, erosion, exhumation and subsidence. The rocks within uplifted normal fault footwall blocks tend to cool down, either as a result of direct tectonic exhumation by removal of the hanging wall, or by erosional exhumation of the uplifted fault block. Meanwhile, the rocks within the subsided hanging wall block are usually heated due to burial, sediment deposition, and/or enhanced heat flow within the rift (Ehlers et al., 2001; Stockli, 2005). The amount of fault slip accumulated may therefore be recorded by the difference in the thermal signature between rocks across the fault boundary. The difference in the thermal signature may become large enough to be resolved by low-temperature thermochronometry and thus be used to place constraints on the timing and magnitude of vertical components of the accumulated fault motions (Ehlers et al., 2001; Stockli et al., 2005).

The understanding of the timing of tectonic processes and associated strain accommodation is important for providing insights into how continental rift systems at their early stages are evolving. This provides more information to understanding the processes and structures associated with tectonic activities along place boundaries. The thorough knowledge of the models of continental rifting at their early stage will help with seismic hazard mitigation as most of the extension along rift basins is accommodated along the major border faults and have the potential to host earthquakes (Foster and Jackson, 1998; Craig et al., 2011, Ebinger et al., 2019). Rift basins are also one of the major locations for hydrocarbon accumulation (Macgregor, 2015). Therefore, it is vital to provide accurate geometry of structures and timing of deformational processes in early-stage continental rifting due to their economic and hazard implications.

CHAPTER II

LITERATURE REVIEW

2.1 Literature Review

The development of continental rifts starts with brittle deformation of the crust by the formation of graben-like bounding faults (Cowie et al., 2005; Ebinger & Scholz, 2012). The rift systems form and evolve in response to the variations in tectonic, crustal, and rheological conditions over time until seafloor spreading processes take over. Narrow rifting starts with continental rifts (e.g. Malawi, Rhine, Baikal or Ethiopian Rifts) and ends up with passive margins and continental break-up (Brun & Choukroune 1983; Buck 1991) while, in wide continental rifts (e.g. the ongoing extension of the North American Cordillera and the Aegean domain), continental thinning occurs over a continental width many times the thickness of the lithosphere and involves intense ductile flow of the lower crust and upper crustal boudinage, facilitated in many cases by the formation of low-angle detachment faults (e.g. Basin and Range; Coney & Harms, 1984, Armijo et al., 1986, Deng et al., 2020). Strain accommodation is usually distributed across the wide rift system and localized mostly along border faults of narrow rift systems.

Extension in the upper crust is accommodated by two types of fault systems: border faults and intra-rift faults. Border faults bound rift segments and accrue kilometers of throw while intra-rift faults are usually smaller than border faults, accrue tens to hundreds of meters of throw,

and form in the inner depressions of rift basins (Corti, 2009). In early stage rifting as in the Malawi Rift,models and field observations suggest about 90% of strain is accommodated along the rift border faults and that intra-basin faults have restricted strain accommodated until later stages of the rift evolution when border faults become mechanically unfavorable for continued slip (Muirhead et al., 2019; Corti, 2009; Ebinger, 2005; Goldsworthy & Jackson, 2001; Scholz & Contreras, 1998). However, Wedmore et al. (2020) suggests that this is not always the case. The authors used observations from strain rate measurements along the Zomba Graben border faults and intra-rift faults to investigate the evolution of an early-stage rift system. Strain is localized along border faults in the first few million years of rifting as asymmetric subsidence to produce graben and half-graben morphologies. During this period, border faults accrue more than 1 km of throw, subsequently induce extension within the rift basins, which are accommodated by formation of intra-rift faults as slip rates of border faults are reduced (Muirhead et al., 2016). Strain accommodation along faults is usually associated with structural, thermal, and chemical alterations of rocks. Some of these alterations are recorded in minerals present in the rocks and these minerals serve as useful tools to investigate the evolution of rift systems.

Thermochronological studies have contributed to understanding the plate boundary evolution and the landscape evolution for more than 35 years (Gallagher et al., 1998; Reiners et al., 2005; Malusà and Fitzgerald, 2019). A good way to study strain accommodation in terms of its thermal changes is through thermochronological analysis to constrain the timing of tectonic processes observed in any geologic unit. The ability to estimate the conditions of formation or alteration of geologic structures at different times in geologic history is an important way to investigate their evolution through time. In the same sense, to understand the evolution of active continental rift systems it is important to investigate the cooling history and corresponding deformation at the border faults along the rift and how it is linked to other rifts. In recent years, low temperature thermochronology like Apatite Fission Track (AFT) has expanded to include

capabilities to investigate areas that have undergone tectonic deformation like uplift, denudation, and tilting (Dekeen et al., 2006). These techniques can investigate the amount of denudation/exhumation, rate and timing of deformation, and invariably the timing of the tectonic processes associated with the strain accommodations observed (Carrapa et al., 2011; Carrapa, 2010). The information on annealing processes derived from AFT length distributions gives this method a further advantage over other thermochronology methods that rely on values of age only.

2.2 Study Area

The Malawi Rift is an approximately 750 km long rift (Ebinger et al., 1989) within the ~4,000 km-long East African Rifts System (EARS). The EARS originated in the Afar Depression in Ethiopia and propagated south as the Main Ethiopia Rift and it split into the western and eastern branches around the Tanzania Craton (Ring et al., 1992). The branch to the west continues to the Malawi Rift in the south. The Malawi rift is believed to have begun propagation in the Rungwe volcanic province and ends against the Shire graben in the south. Specht and Rosendahl, (1989) showed the trend of propagation of the Malawi rift using the thickness of the sedimentary fill of the rift. The authors observed through seismic imaging that the sedimentary fill thickness becomes thinner southwards in the rift. About 2 to 3 km of sediment thickness is observed in the north of the rift while the thickness is gradually decreasing towards the south as the rift terminates against the Shire Graben (Figure 1). The Malawi Rift can be sub-divided into 8 distinct full grabens and half grabens of about 100 –150 km length with the orientation alternating along its axis (Laó-Dávila et al., 2015).

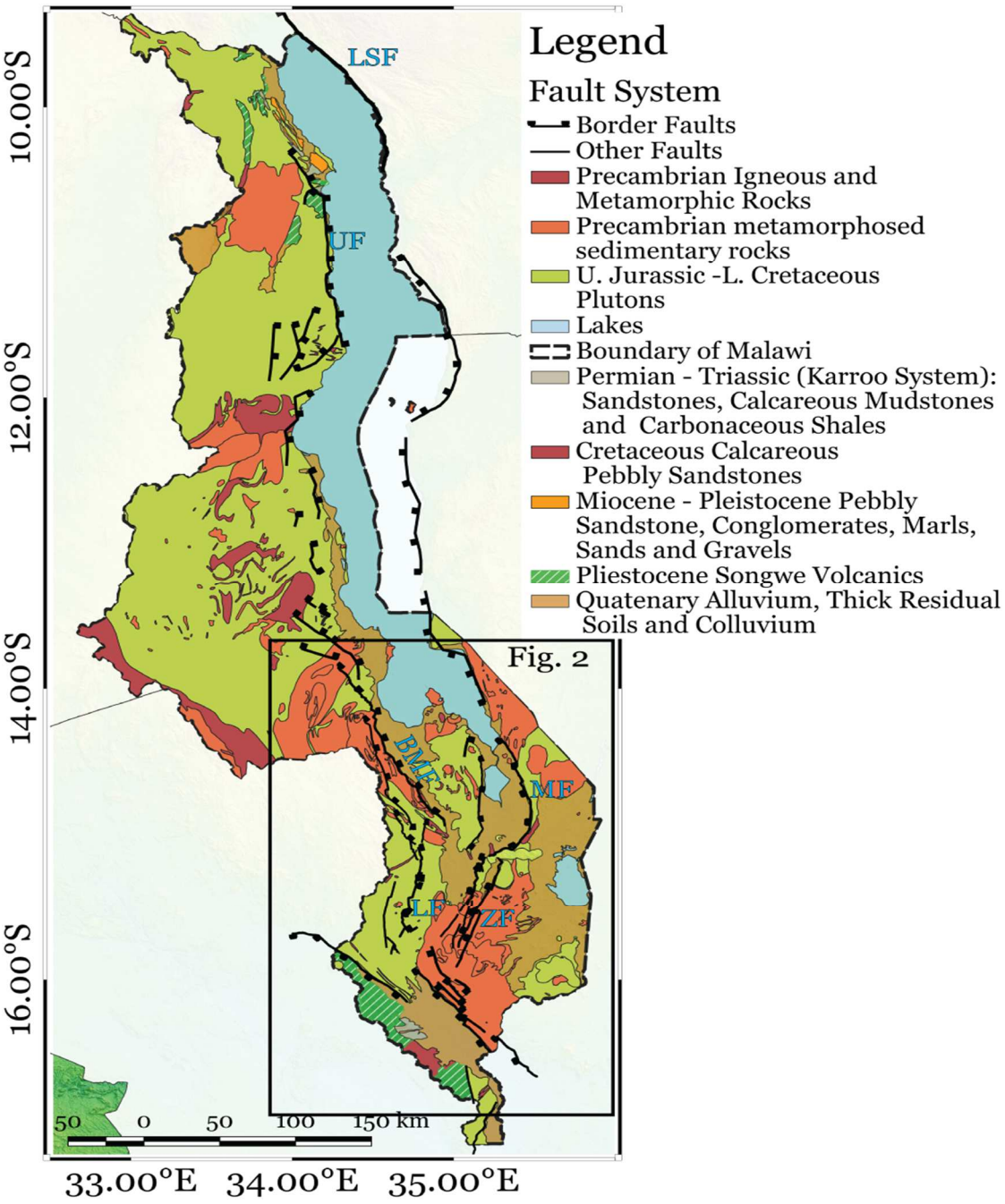

Figure 1: Geologic and structural map of the Malawi Rift and Shire Rift highlighting the major border faults. (Modified from Bloomfeld et al., 1965) LSF – Livingstone Fault, UF – Usisya

Fault, MF – Mwanjage Fault, ZF – Zomba Fault, BMF – Bilila-Mtakataka Fault, LF – Lisungwe Fault.

The southern Malawi Rift covers southern segments in the hierarchal segmentation of the Malawi Rift (Laó-Dávila et al., 2015). The major grabens and some associated major border faults in the southern Malawi Rift are the Makanjira graben (Bilila-Mtakataka Fault (BMF), Malombe Fault (MB), Zomba Graben (Zomba Fault (ZF), Lisungwe Fault (LF)) and some border faults associated with the grabens in the southern Malawi Rift include Thyolo and Muona faults (Figure 2).

The ages of the tectonic deformation of the region were established through the recognition of correlations between the deformation, emplacement of magmatic bodies and sedimentation (Castaing, 1991). Castaing, (1991) identified three major episodes of tectonic activities as the Karoo rifting period (Late Carboniferous to Early Jurassic), the post-Karroo alkaline igneous activity (Middle Jurassic to Cretaceous) and the East African Rift System (Cenozoic to Recent). Orientations of each of the tectonic events were established from structural analysis of the fracture systems (Castaing, 1991).

Certain parts of the Malawi rift have AFT ages to evaluate the tectonic and denudation history, uplift and isostatic rebound of the footwall blocks, and deformation associated with igneous intrusions (Eby et al., 1995; Van Der Beek et al., 1998; Dazinnes et al., 2011; Mortimer et al., 2016). Van Der Beek et al., (1998) used inverse modelling of fission track measurement distributions to reconstruct a thermal history that suggests distinct repeated phases of uplift and denudation of the rift flanks along the Livingstone Fault in the northern part of the Malawi Rift at 250–200 Ma, 150 Ma, and 140–50 Ma. Mortimer et al., (2016) adopted low-temperature apatite (U–Th)/He (AHe) to investigate the along-strike and vertical distribution of cooling ages along

the Livingstone fault, the bounding fault system of the Karonga Basin of the northern Malawi Rift. Thermochronological investigation of the Livingstone fault by Mortimer et al., (2016) reveals from age-elevation relationships that regional-scale cooling associated with Cenozoic rifting of the Malawi Rift began at ~23 Ma and that low-temperature (A-He) thermochronology can record segmentation and linkage of border faults. Eby et al., (1995) and Dazinnes et al., (2011) used AFT to estimate the age of the igneous intrusions in the Chilwa Province of southern Malawi along the rift shoulders. Even though these contemporary studies mentioned above have provided insight into some tectonics of continental rift, there remains a knowledge gap in the thermochronological and tectonic history of early-stage rifting in the Southern Malawi Rift and this study addresses it.

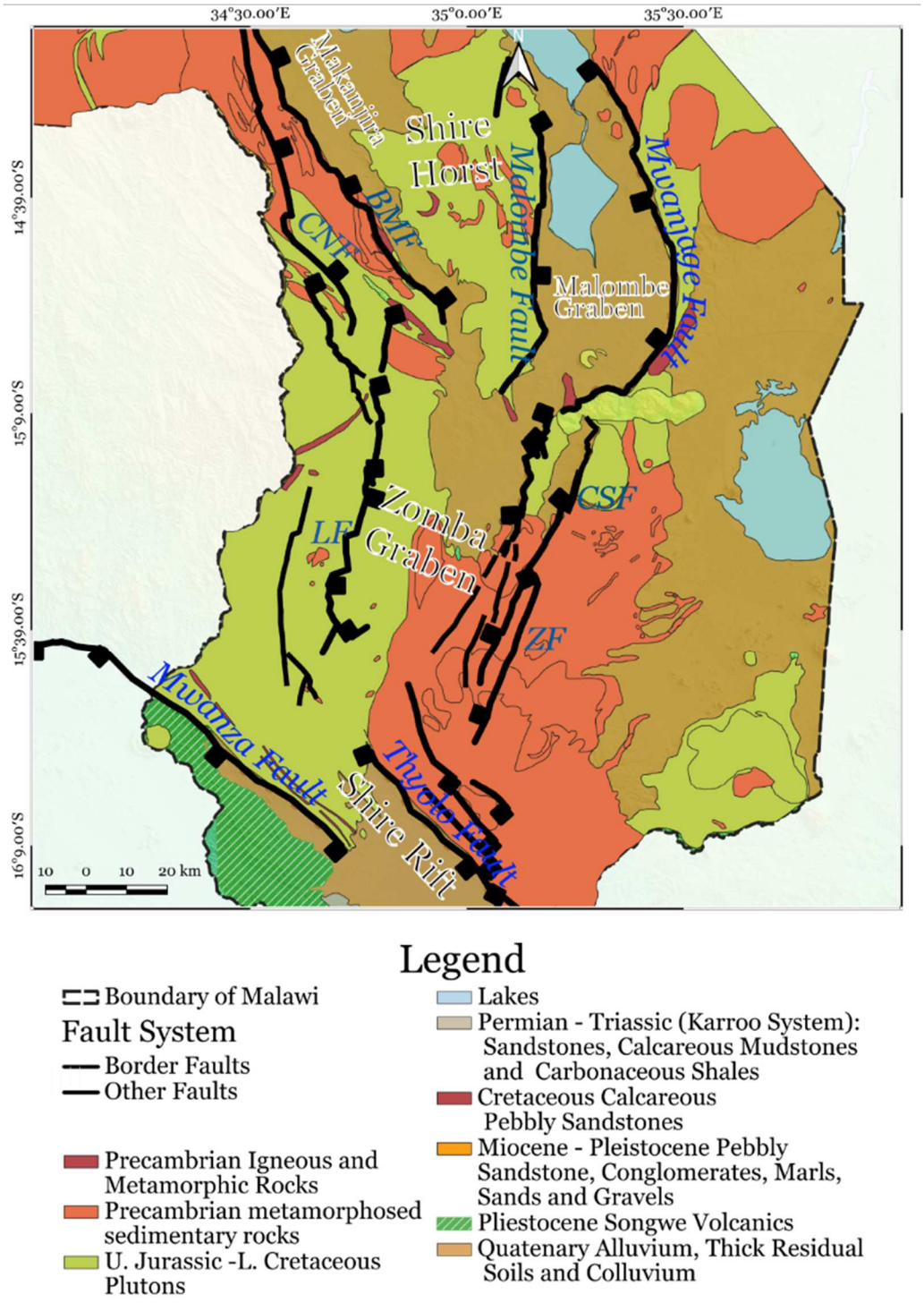

Figure 2: Geologic map of the study area, which includes the southern Malawi Rift and Shire Rift, showing the different geologic units and the major fault systems.

CHAPTER III

METHODOLOGY

We applied remote sensing and low temperature thermo-geochronology to understand the interaction between timing and tectonic uplift during the evolution of the southern part of the Malawi Rift and the northern Shire Rift. Geochronologic studies using Apatite Fission Track (AFT) measurements were carried out. This includes apatite mineral separation, fission tracks mounting and measurement. These were used in determining the cooling ages along the footwall blocks of the Rift from AFT and also the estimation of the depth of formation of AFT to infer fault throw and estimate fault displacement and extension. The geometry of structures along the Southern Malawi Rift and Shire Rift were also investigated by remote sensing analysis of satellite data by using hillshade imaging and slope analysis of satellite data (SRTM-DEM).

3.1 Apatite Fission Track Measurements

The application of FT thermochronology is well-established in extensional tectonic settings where cooling is a product of both tectonic footwall exhumation, and through erosional exhumation of uplifted footwall blocks (Fitzgerald et al. 1991; Foster et al. 1991; Ehlers et al. 2001; Stockli, 2005). Here we have applied apatite FT dating to investigate the timing and magnitude of upper crustal (2-5 km; 60–130 °C) cooling and exhumation ages associated with

footwall uplift on 13 rock samples (gneisses, syenite, foliated granite, and granite dikes) collected from the footwall blocks of several major extensional border faults (Fig. 2). Mineral separation was undertaken at Zirchron LLC, Geoscience Services using electro pulse disaggregation. The fission track mounting, calibration, and measurement were done at the University of Arizona Fission Track Laboratory. Apatite sample irradiation was carried out at the Oregon State University Radiation Center.

The FT ages were measured by using the External Detector Method (EDM). The external detector methods for fission-track (FT) thermochronology are based on a combination of zeta calibration against independent age standards. This method involves calculating the spontaneous track density in a selected grain and finding the exact mirror image of the counted area on the corresponding muscovite/mica external detector where the induced track density is counted over the same area. A geometry factor of 0.5 was used to correct for difference in the geometry of track registration for the internal surface on which the spontaneous tracks are measured and the external detector surface used for induced tracks, (e.g., Wagner and van den Haute 1992). Apatite crystal grains were carefully selected, with only grains with the highest etching efficiency (parallel to the c-axis) selected for counting and horizontal confined track length measurement (e.g., Gleadow 1978). Apatite fission tracks anneal at low temperatures between 130–60° C over geologic timescales and thus record the thermal history of samples subject to tectonic processes of brittle deformation taking place in the upper continental crust (~2–5 km).

3.2 Inverse thermal history modelling

A given fission track length distribution can be related quantitatively to a thermal history, using a mathematical description of the annealing process (e.g. Ketcham et al. 2007). Therefore,

the lengths of horizontal confined fission tracks were measured in each of the samples to help constrain the thermal history that most-likely predicts the measured data using inverse thermal modeling software HeFTY version 1.9.3 (Ketcham, 2005), the apatite FT annealing model of Ketcham et al. (2007), and Dpar (etch-pit diameter parallel to the c-axis) as an additional kinetic parameter. Laboratory experiments show that the thermal annealing of fission tracks in apatite obeys a so-called fanning Arrhenius relationship, in which the degree of shortening depends on both the amount and duration of heating. The HeFTy program uses a Monte Carlo method that generates FT data from large numbers of thermal histories according to the Ketcham et al. (2007) apatite FT annealing model and uses the p value of formalized hypothesis tests like the chi-square test to assess the goodness of fit of the model predicted data with the measured data, and thus decide which t–T paths to retain or reject. We used 20 ± 5°C as present day temperature, two constraint boxes, and default values for other parameters for inverse modelling of all the samples. The first main constraint box covers 5-200 Ma, 20-180°C to account for tectonic events which include the Gondwana breakup and subsequent Karoo rifting, alkaline igneous intrusions, and the more recent East African rifting, that span this geologic time (Castaing, 1991; Eby et al., 1995). 30 - 0.1 Ma and 20 - 100°C were used for the second constraint box to help provide more details and constraint points on more recent cooling history (Castaing, 1991; Van Der Beek et al., 1998; Mortimer et al., 2016). The second constraint box is to provide more details on the thermotectonic history of the East African rifting along the Malawi Rift which has been constrained and suggested to have initiated around this time in the region.

The advantages of the FT method over other techniques when applied to fault zones are that more apatite mineral grains can be used for FT analysis within continental crust rocks, providing greater thermal sensitivity for secondary heating episodes associated with faulting. (Ehlers et al., 2001; Stockli, 2005). We accounted from known issues including the effects of

near-surface processes like topographic relief, lightning, and wildfires (Peyton and Carrapa, 2013) through careful selection of samples which have been least affected by some of the processes mentioned above, from the large group of samples originally collected from another research project in southern Malawi in 2016.

3.3 Remote Sensing Analysis

Analysis was carried out on a 30-m resolution Shuttle Radar Topography Model (SRTM) digital elevation model (DEM) using QGIS and ENVI software to map major fracture systems of the study area. A hillshade map was created from the SRTM-DEM using the sun angle of 45^{o} and azimuth of 315^{o} to highlight the major faults in the study area as it produces the topographic view of the terrain from elevation data. Geologic structures can be easily mapped from the hillshade map superimposed with a pseudocoloured DEM to illustrate the variations in elevation across the rift system. We measured and interpreted orientation of regional fractures and minimum scarp heights of major border faults which are essential parameters in delineating tectonic conditions from the mapped faults.

A slope map was also created from SRTM-DEM using QGIS. Slope analysis was done to also delineate the geologic structure along the accommodation zone between the Southern Malawi Rift and Shire Rift. The pattern of change in slope or dip of geologic structures provide important information on the tectonic setting and architecture of the structures at the surface. Structures like relay ramps which are usually found across accommodation zones are indicative of linkage and transfer of strain between geologic structures. Relay ramps that have breached have been established to have certain dip or slope (10 – 15^{o} for recently breached relay ramps) and this will help in structurally characterizing this region for structures that could facilitate strain transfer (Fossen and Rotvatn, 2016 and references therein).

For structural characterization of the fracture systems, SRTM-DEM hillshade and slope maps from satellite data of the study area were used to map fracture systems along the rift border faults. The SRTM-DEM hillshade and slope analyses provided information about the geometry of fracture systems in the area. The mapped fractures from the hilshade and slope maps combined with faults mapped from previous studies (Kolawole et al., 2021) were used to generate a density plot of the fracture systems along the accommodation zone between the southern Malawi Rift and the Shire Rift. The density plot of the fractures can help determine the model of rift linkage (Brune et al., 2017) and potential for strain transfer can be interpreted and inferred from the geometry.

3.4 Estimation of Strain Rates along Southern Malawi Rift vs Northern Malawi Rift

Exhumation is the vertical motion of a rock towards the Earth surface (England and Molnar, 1990). We estimated the extension and displacement which are forms of strain and the respective strain rates (extension rates and slip rates) from the uplift or exhumation (vertical motion of a rock perpendicular the Earth surface) calculated from our AFT modelling of the samples (Fitzgerald and Malusa, 2019). It becomes useful in estimating the extension and displacement along fault if the heave or dip of the fault is known. Effective constraints on the timing of the uplift, which could be estimated from AFT measurements and modelling, makes it possible to determine the strain rates which are vital to understanding strain accommodation along early-stage continental rift systems. Temporal constraints on exhumation were directly established by the cooling ages that are set during undisturbed cooling across the closure temperature isothermal surface. Sometimes however, cooling may not be related to exhumation, but can be used instead to constrain the thermal evolution of the upper crust and the emplacement depth of magmatic rocks. For example, if magma is emplaced at

shallower crustal levels compared to the undisturbed isothermal surface (Tc) observed before intrusion, magmatic rocks will cool after intrusion at temperatures below Tc without moving towards the Earth's surface (often referred to as thermal relaxation), and thus provide no direct constraint on exhumation along the border faults (Malusà et al. 2011). AFT analysis can thus be used both constrain exhumation, and/or to constrain the thermal evolution of the upper crust and the emplacement depth of magmatic rocks, with differentiation between the two cooling processes reliant on appropriate consideration of the age and extent of the local magmatic history of the study area.

We calculated an average exhumation rate using a single sample. In order to calculate an average exhumation rate from a single sample, the paleo-geothermal gradient i.e. the vertical distance between the Tc and Earth's surface during exhumation has to be independently known. The average exhumation rate was calculated from the time of cooling across the Tc isothermal surface to the time of final exposure of the sample to Earth's surface (e.g., Wagner et al. 1977). Generally, geothermal gradient of 25 – 30^{o} C/km is assumed for most tectonic settings across the surface of the Earth and this has also been determined by Van Der Beek et al., (1998) from heat flow in the Earth crust across the northern Malawi Rift as 25 – 30^{o} C/km. Cooling rates were converted to exhumation rates assuming a geothermal gradient.

The strain accommodated in the southern Malawi Rift was calculated using the relationships shown in equations 1 and 2 below;

$$\text{Displacement} = \frac{\text{Uplift}}{\sin\alpha}; \qquad Heave = \frac{Uplift}{\tan\alpha} \qquad \text{Eqn. 1}$$

Where α is the dip of the fault (assumed to be 45^{o}, 60^{o} or 75^{o} for the Malawi Rift) (Muirhead et al., 2016).

Using eqn. 1 above and timing constrained from AFT modelling, the strain rates for the southern Malawi Rift is calculated as;

$$\text{Strain Rate} = \frac{\text{Strain}}{\text{Time}} \qquad \text{Eqn. 2}$$

CHAPTER IV

FINDINGS

4.1 Apatite Fission-Track Age Measurements

We summarize the thermochronologic data from the Southern Malawi Rift and Shire Rift and integrate it with geologic constraints to determine evolution of these two continental rift systems in terms of strain accommodation in the upper crust (2-5 km depth) spanning about 135 Ma. AFT central ages range between 60 ± 4 Ma and 128 ± 6 Ma, while mean track lengths (MTLs) range between 13.35 μm and 11.02 μm (Table 1 and 2). AFT ages show no obvious trend versus elevation, although given the large geographic spread and small elevation difference between samples this is to be expected. Age against distance along rift strike do not seem to show a trend of younger ages near the southern fault tips. Our results are consistent with previous studies by Eby et al., (1995) and Daszinnies et al., (2008; 2009) who measured AFT ages of the alkaline igneous intrusions and along the rift shoulders of the southern Malawi Rift as it cuts across Malawi and Mozambique. The range of cooling ages from these previous studies and that of this study along the rift's border fault scarp appears to be close. (Fig. 3).

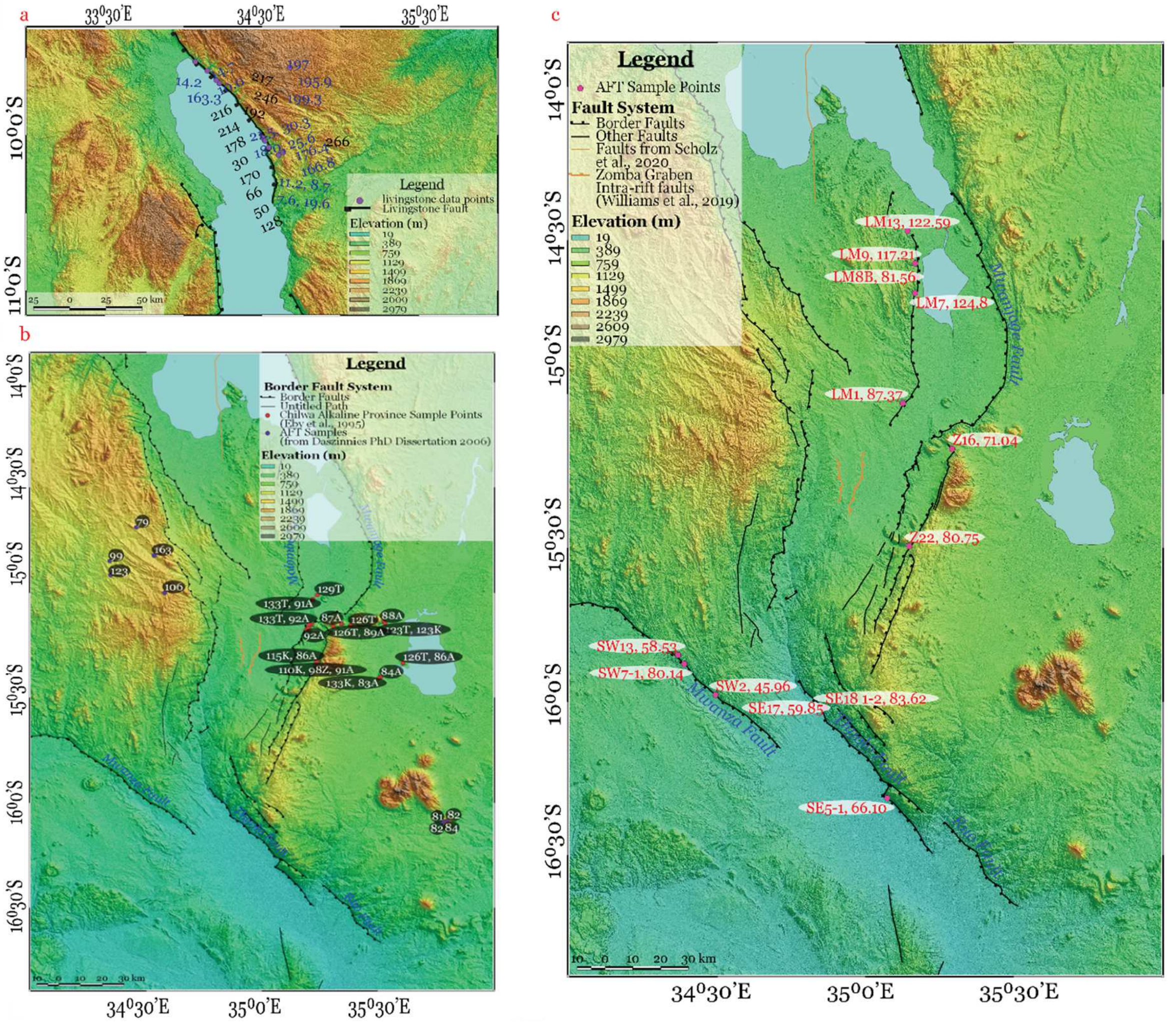

Figure 3: (a) Hillshade Map of the Malawi Rift showing both the southern and northern Malawi Rift. (b) Map of southern Malawi Rift showing the major border faults highlighted and the location of the samples collected for this study and samples from Eby et al (1995) with corresponding AFT (A), K/Ar (K) and Titanite (T) ages in millions of years. The intra-rift faults highlighted in brown are from Wedmore et al., (2020). Dashed-line rectangle shows area of remote sensing study.

Table 1: Fission-track Data

Sample	*No. of Crystals*	*Track Density (x 106 tracks.cm-2)*			*Age Dispersion*	*Central Age (Ma)*	*Apatite Mean Track Length*	*Standard Deviation*
		ρs (Ns)	*ρi (Ni)*	*ρd (Nd)*	*(Pχ2)*	*(±1σ)*	*(μm ± 1 s.e.) (no. of tracks)*	*(μm)*
LM 1	20	2.295 (2446)	6.458 (6882)	1.608 (5145)	10.6% (0.16%)	**87.4±4.1**	**13.01±0.16 (99)**	**1.55**
LM 7	20	2.341 (1516)	4.532 (2935)	1.594 (5101)	3.5% (47.3%)	**124.8±5.6**	**12.43±0.16 (101)**	**1.60**
LM 8B	20	2.902 (302)	0.8543 (889)	1.580 (5057)	1.4% (64.9%)	**81.6±6.0**	**12.94±0.12 (100)**	**1.21**
LM 9	20	1.138 (1413)	2.318 (2878)	1.566 (5013)	12.8% (0.99%)	**117.2±6.3**	**12.15±0.16 (100)**	**1.63**
LM 13	20	1.519 (1750)	2.844 (3276)	1.553 (4969)	23.3% (<0.01%)	**122.6±8.4**	**11.94±0.18 (101)**	**1.84**
SE 5-1	20	0.602 (482)	2.130 (1705)	1.539 (4925)	(5.93%) (64.24%)	**66.08±4.11**	**11.02 ± 0.18 (98)**	**1.82**
SE 17	20	0.3540 (389)	1.381 (1518)	1.525 (4480)	13.2% (17.2%)	**59.9±4.3**	**12.33±0.15 (100)**	**1.51**
SE 18-1-2	20	0.4424 (310)	1.214 (851)	1.511 (4836)	0.03% (88.3%)	**83.6±6.1**	**13.18±0.14 (104)**	**1.44**
SW 2	20	0.09723 (85)	0.2883 (252)	1.382 (4422)	<0.01% (99.8%)	**79.5±10.2**	**-**	**-**
SW 7-1	20	0.5927	1.670	1.484	8.3%	**80.1±5.7**	**12.74±0.10**	**1.02**

		(374)	(1054)	(4748)	(36.1%)		**(100)**	
SW 13	20	0.2474	0.9389	1.470	26.1%	**58.5±6.8**	**12.83±0.18**	**1.63**
		(146)	(554)	(4704)	(10.7%)		**(81)**	
Z 16	20	0.3465	1.080	1.456	<0.01%	**71.0±4.8**	**13.35±0.12**	**1.19**
		(361)	(1125)	(4660)	(99.8%)		**(100)**	
Z 22	20	2.283	6.193	1.442	0.75%	**80.8±3.8**	**12.49±0.15**	**1.51**
		(1081)	(2933)	(4616)	(58.2%)		**(107)**	

Notes:
(i). Analyses by external detector method using 0.5 for the $4\pi/2\pi$ geometry correction factor;
(ii). Ages calculated using dosimeter glass: IRMM540R with ζ_{540R} = 305.8±8.4 (apatite);
(iii). $P\chi^2$ is the probability of obtaining a χ^2 value for v degrees of freedom where v = no. of crystals - 1;
(iv). s.e. = Standard Error.

Table 2: AFT Sample Location and Elevation data

Samples	***Latitude***	***Longitude***	***Elevation (m)***
Malombe Fault			
LM 9	-14.574	35.167867	598
LM 1	-15.0297	35.126611	539
LM 7	-14.6709	35.1676	579
LM 8B	-14.6169	35.17185	576
LM 13	-14.4687	35.1418	579
Chingale-Step Fault			
Z 16	-15.1779	35.293267	803
Z 22	-15.4938	35.1476	773
Thyolo Fault			
SE 5-1	-16.3134	35.073833	201
SE 18 1-2	-16.0193	34.863583	335
SE 17	-16.0198	34.8608	305
Mwanza Fault			
SW 7-1	-15.8764	34.387933	306
SW 2	-15.9788	34.493583	247
SW 13	-15.8475	34.367233	495

4.2 Outcomes of Thermochronological Data Modelling

The relationship of between the fission track ages and the mean confined track lengths for each sample are shown in a boomerang plot (Green, 1986; Gleadow et al., 1986) in Figure 4. With the exception of sample SE 5-1, the data show most relatively short mean track lengths (< ca. 13 μm) that show a general trend of increasing mean lengths with decreasing age. Such a pattern allows a qualitative assessment of the thermal history of these samples (e.g. Gallagher and Brown, 1997) indicating a cooling episode in the last ca. 50 million years (younger than the youngest AFT age) from temperatures within the AFT partial annealing zone (ca. 60-120 °C). Results from thermal history modelling using HeFTy software are shown for the southern Malawi Rift (Figure 5 and 6) and the Shire Rift (Figure 7 and 8).

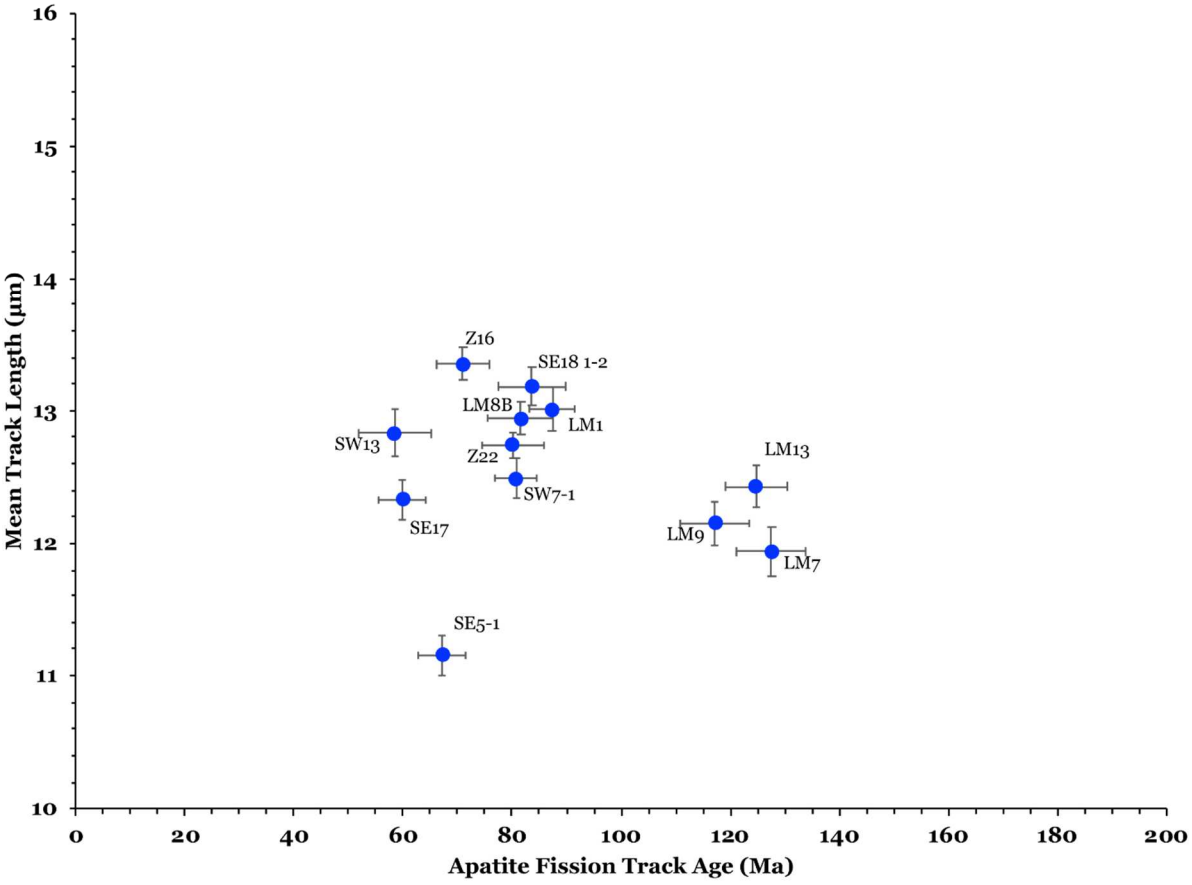

Figure 4: showing the relationships between the estimated AFT ages (Ma) vs the measured confined mean track lengths for each of the 12 samples used for the thermal modelling of the cooling history in this study. One sample (SW2) was omitted because of the lack of confined fission tracks in the sample.

4.2.1 *The southern Malawi Rift*

The southern Malawi Rift incorporates seven samples and seven thermal histories from the rift border faults. A thermal history path for all the samples along the Malombe Fault and Chingale-step Fault exhibit three periods of cooling.

Malombe Fault shows an initial protracted rapid cooling period between 100 and 80 Ma. (2.0 °C/Ma.), followed by slow cooling from 80 Ma to 20 Ma. (0.33 °C/Ma.), a period of rapid protracted cooling since 20 - 5 Ma (1.6 – 2.66 °C/Ma) (Fig. 5).

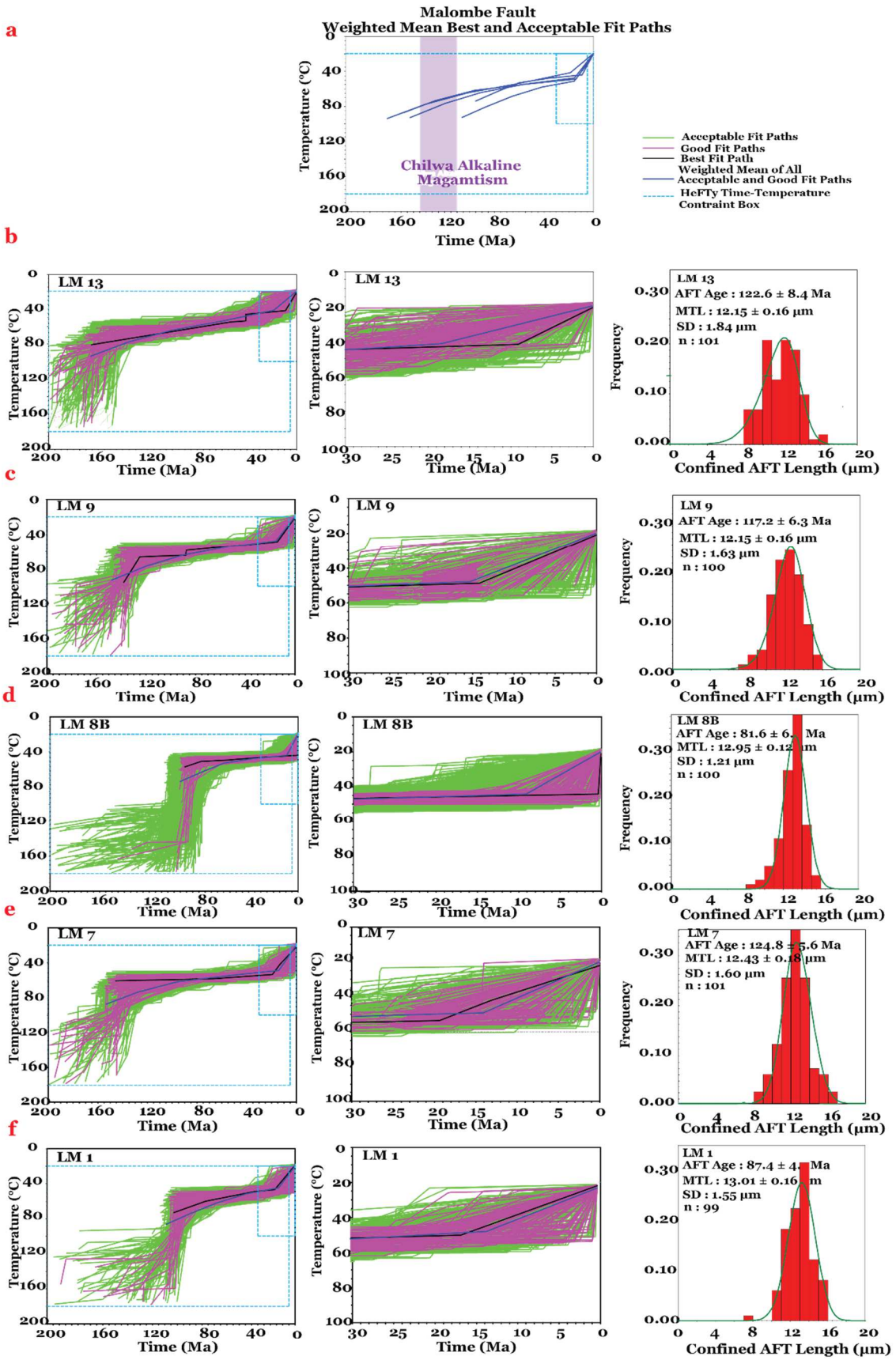
a
Malombe Fault
Weighted Mean Best and Acceptable Fit Paths
Temperature (°C)
Time (Ma)
Chilwa Alkaline Magamtism
Acceptable Fit Paths
Good Fit Paths
Best Fit Path
Weighted Mean of All Accceptable and Good Fit Paths
HeFTy Time-Temperature Contraint Box
b
LM 13
AFT Age : 122.6 ± 8.4 Ma
MTL : 12.15 ± 0.16 µm
SD : 1.84 µm
n : 101
Frequency
Confined AFT Length (µm)
c
LM 9
AFT Age : 117.2 ± 6.3 Ma
MTL : 12.15 ± 0.16 µm
SD : 1.63 µm
n : 100
d
LM 8B
AFT Age : 81.6 ± 6.
MTL : 12.95 ± 0.12
SD : 1.21 µm
n : 100
e
LM 7
AFT Age : 124.8 ± 5.6 Ma
MTL : 12.43 ± 0.18 µm
SD : 1.60 µm
n : 101
f
LM 1
AFT Age : 87.4 ± 4
MTL : 13.01 ± 0.16
SD : 1.55 µm
n : 99

Figure 5: Thermal history models from the southern portion of the Malawi Rift (Makanjira Graben and Malombe Fault) with age and track length distribution prediction outlined. The black line within each thermal history is the path of best fit for the expected model and the green paths outlines the acceptable paths, weighted mean of all acceptable and good fit paths is shown with the blue line and the pink paths are the good paths that best predicts the thermal histories. The figures for each sample are arranged from north to south. (b) LM 13, (c) LM 9, (d) LM 8B, (e) LM 7, and (f) LM 1.

Chingale-step Fault shows an initial protracted rapid cooling period between 90 and 75 Ma. (5.33 °C/Ma.), followed by slow cooling from 70 Ma. to 5 Ma. (0.15 °C/Ma.), a period of rapid protracted cooling since about 5 Ma (2 °C/Ma.) (Fig. 6)

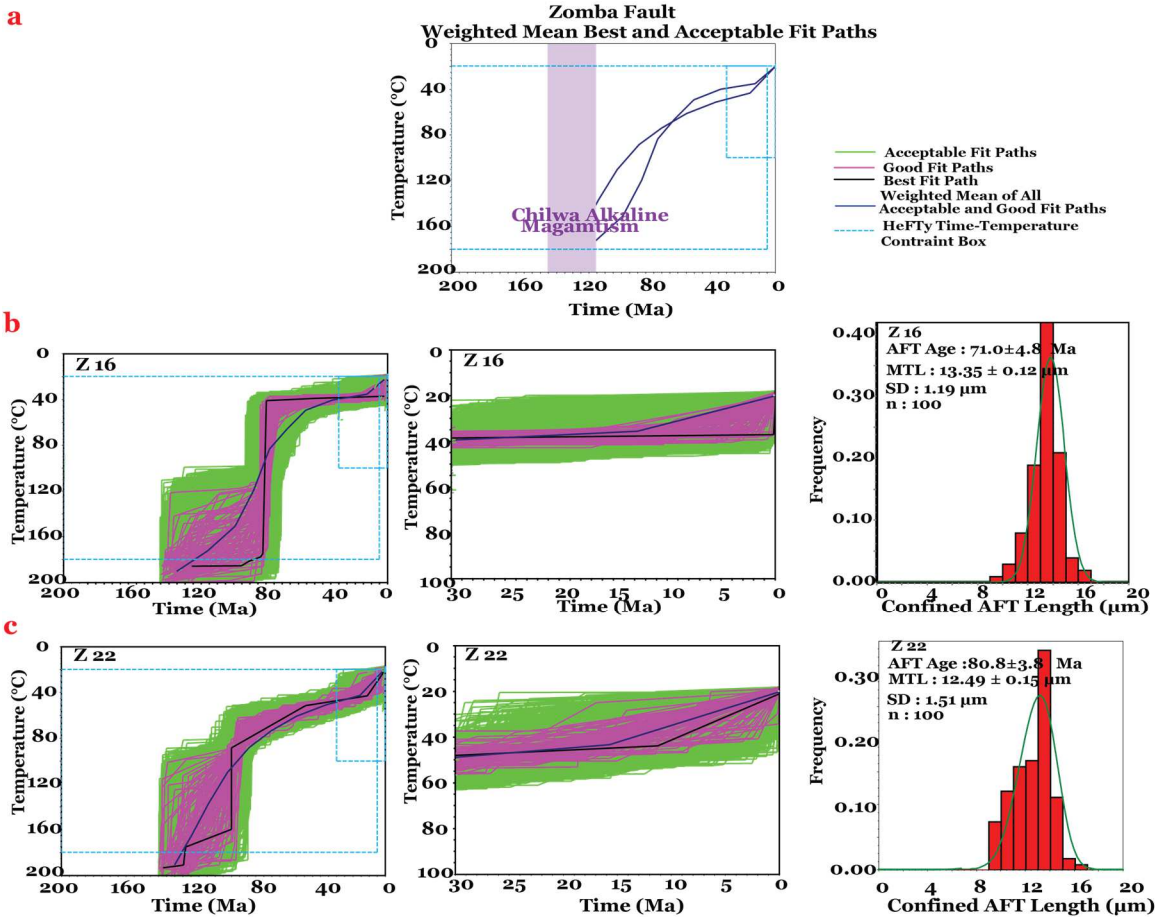

Figure 6: Thermal history models from the southern portion of the Malawi Rift (Zomba Graben; Chingale-step Fault) with age and track length distribution prediction outlined. The black line within each thermal history is the path of best fit for the expected model, weighted mean of all acceptable and good fit paths is shown with the blue line and the green paths outlines the acceptable paths and the pink paths are the good paths that best predicts the thermal histories. (a) Z16, and (b) Z22.

4.2.2 The Shire Rift

The Shire Rift incorporates five samples, 4 taken along the rift border fault scarps and 1 from the rift shoulder. Thermal histories outline relatively 3 distinct episodes of cooling rate (Fig. 7 and 8).

Thyolo Fault shows an initial protracted rapid cooling period between 90 and 65 Ma. (2.8 °C/Ma.), followed by slow cooling from 60 Ma to 20 Ma. (0.5 °C/Ma.), a period of rapid protracted cooling since 20–5 Ma (1.6–2.66 °C/Ma.) (Fig. 7).

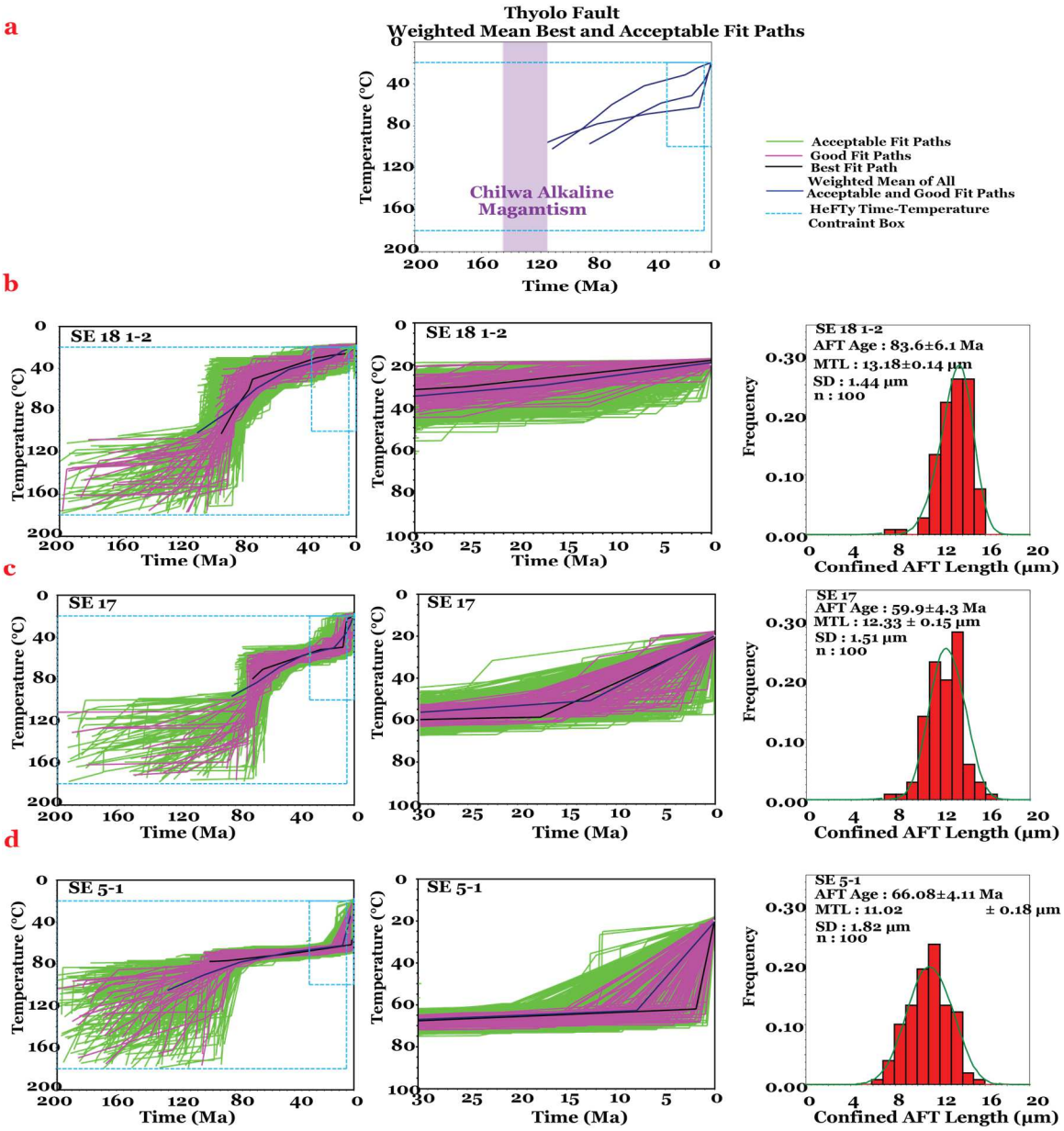

Figure 7: Thermal history models from the northern portion of the Shire Rift (Thyolo Fault) with age and track length distribution prediction outlined. The black line within each thermal history is the path of best fit for the expected model and the green paths outlines the acceptable paths, weighted mean of all acceptable and good fit paths is shown with the blue line and the pink paths are the good paths that best predicts the thermal histories.

The Mwanza Fault could not be effectively constrained through thermal modelling due to low uranium content and corresponding lack of sufficient confined track length data from the samples. The Mwanza Fault shows an initial protracted rapid cooling period between 100 and 80 Ma. (4.5 °C/Ma.), followed by slow cooling from 70 Ma to 5 Ma. (0.46 °C/Ma.), a period of rapid protracted cooling since 5 Ma (2 °C/Ma.) (Fig. 8).

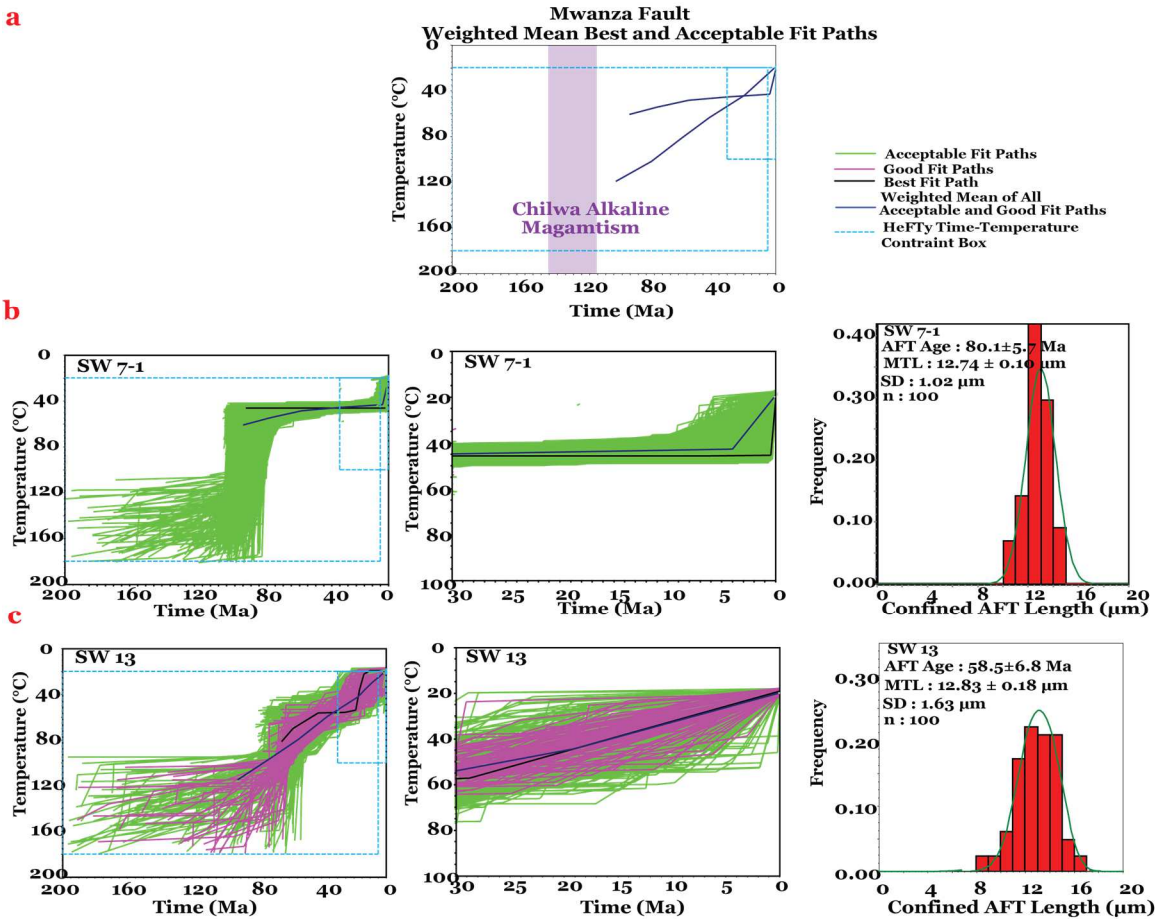

Figure 8: Thermal history models from the northern portion of the Shire Rift (Mwanza Fault) with age and track length distribution prediction outlined. The black line within each thermal history is the path of best fit for the expected model, weighted mean of all acceptable and good fit paths is shown with the blue line and the green paths outlines the acceptable paths and the pink paths are the good paths that best predicts the thermal histories. (a) sample SW7, and (b) sample SW13.

Using this geothermal gradient, our results suggest that the southern Malawi rift has undergone a rapid uplift of about 2 km along the border faults within the last 5 Ma. or so. The Thyolo fault of the Shire Rift also show indications that it has accumulated strain in terms of uplift in the last 5 Ma. of a magnitude of about 2 km also. This further solidifies our observations from fault geometry, cooling age and history with all points towards rift linkage and transfer of strain across the accommodation zone between this rift systems of different origins.

4.3 Remote Sensing Analysis

Analysis carried out on a 30-m resolution Shuttle Radar Topography Model (SRTM) digital elevation model (DEM) using QGIS and ENVI software to map major fracture systems of the study area is shown in Figure 9 and 10. For structural characterization of the fracture systems, slope analysis (Figure 9) and SRTM-DEM hillshade maps (Figure 10) of the study area show fracture systems along the accommodation zone between the Malawi Rift and the Shire Rift. The SRTM-DEM data analysis provided information about the geometry of fracture systems in the area. The mapped fractures show the pattern/model of rift linkage (Brune et al., 2017) and potential for strain transfer will be interpreted and inferred from the geometry.

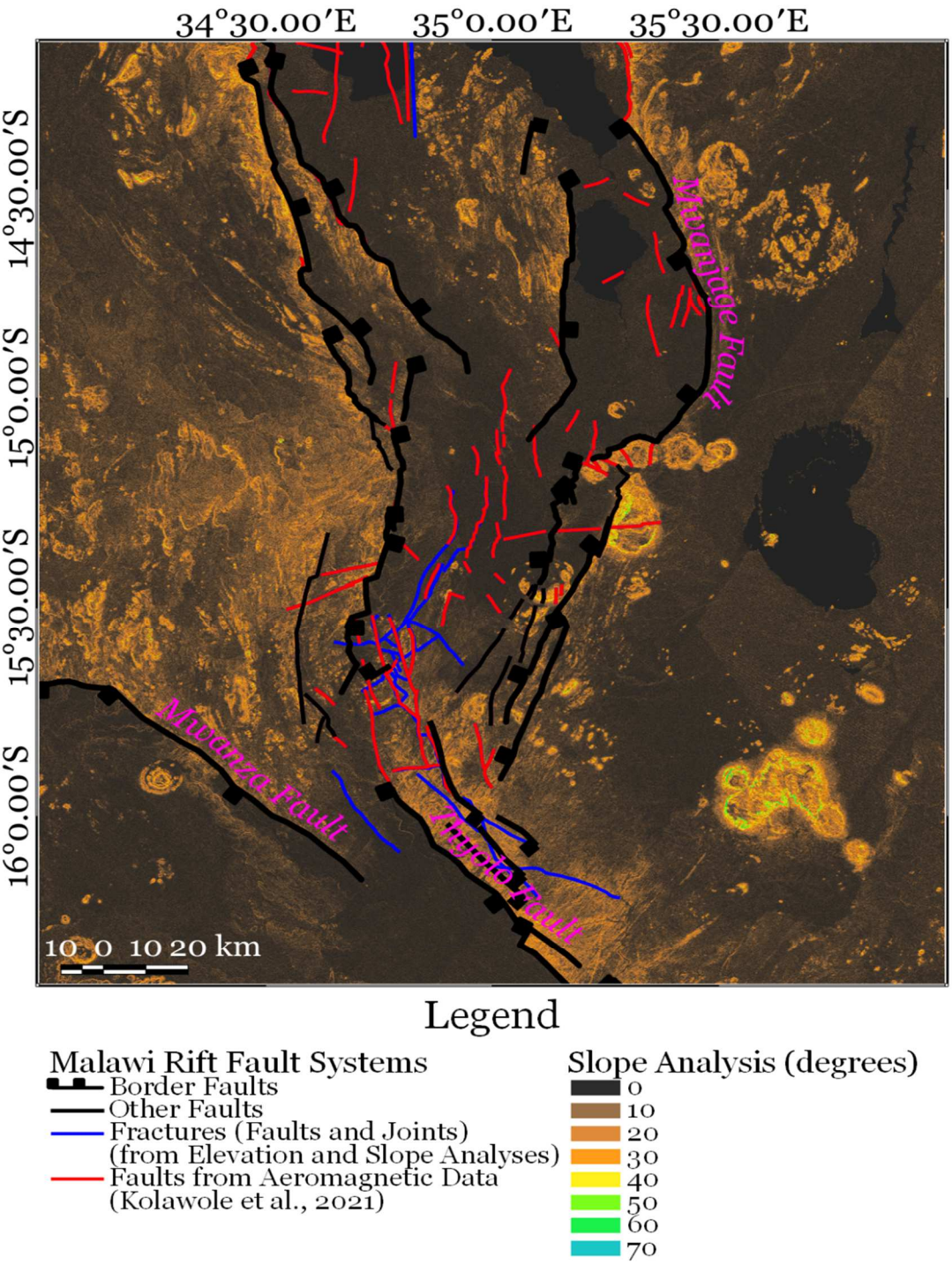

Figure 9: Slope analysis map overlain by some of the fracture systems mapped across the accommodation zone between the southern Malawi Rift and Shire Rift (Modified after Kolawole et al., 2021)

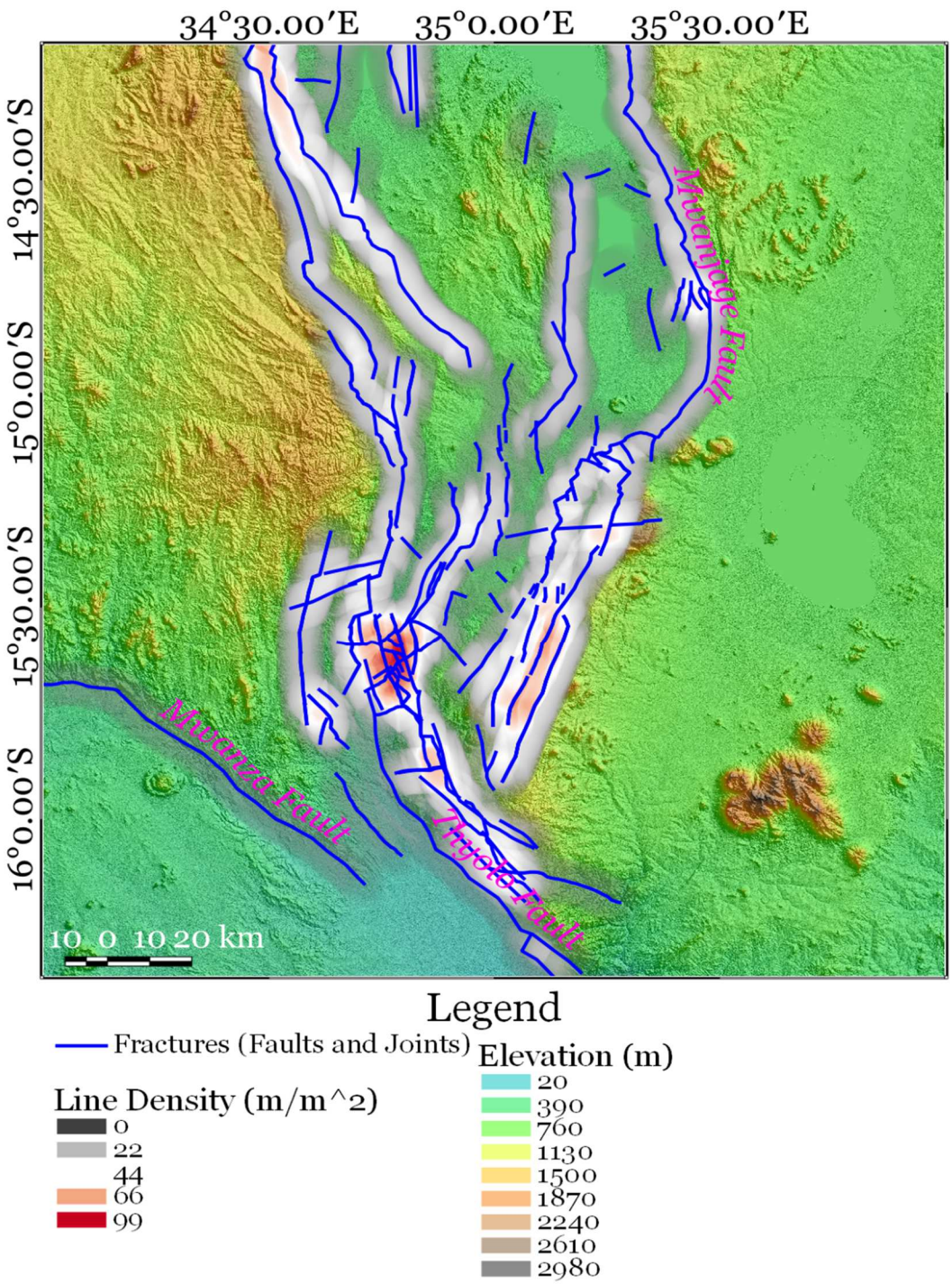

Figure 10: Hillshade map overlain by some of the fracture systems mapped and the respective density plots of the fractures across the accommodation zone between the southern Malawi Rift and Shire Rift

4.4 Strain Rates

The strain rates estimated for southern Malawi Rift from new data acquired for this study and for northern Malawi Rift from previous studies (Van Der Beek et al., 1998; Mortimer et al., 2016; Accardo et al., 2018) are shown in the table below.

Table 3: showing the estimation of strain rates across the southern Malawi Rift and northern Malawi Rift

	Uplift/Throw of Border Faults (km)	Displacement (km)			Strain Rates						
		Heave/Extension (km)			Timing of Uplift (Ma)	5			20		
Fault Dip		45°	60°	75°		45°	60°	75°	45°	60°	75°
Southern Malawi Rift	2.00	2.83	2.31	2.07	Slip Rate (mm/yr)	0.57	0.46	0.41	0.14	0.12	0.10
		2.00	1.15	0.54	Extension Rate (mm/yr)	0.40	0.23	0.11	0.10	0.06	0.03
Northern Malawi Rift (Livingstone Fault)	6.40	9.05	7.39	6.63	Slip Rate (mm/yr)	1.81	1.48	1.33	0.45	0.37	0.33
		6.40	3.70	1.71	Extension Rate (mm/yr)	1.28	0.74	0.34	0.04	0.19	0.09

CHAPTER V

DISCUSSION

5.1 Thermochronological Studies

The results revealed different scenarios of what the cooling ages are and plausible interpretations of the cooling history. The AFT ages indicate the last time a major tectonic event altered the structures of rift. Miocene cooling episodes indicate the effects of faulting associated with East Africa Rift System, footwall uplift or denudation/erosion. Pre-Cenozoic cooling episodes which could be from Cretaceous to Early Permian suggest a series of events that spans from tectonic activities associated with Karoo Rifting (i.e., normal faulting and volcanism) during the Permian to Early Jurassic to Alkaline Complexes (i.e. magmatism during the Cretaceous) (Castaing, 1991). The thermal histories of the samples along the border faults of Southern Malawi Rift and Shire Rift showed some similarities and disparities in the various tectonic and thermal events that these two rift systems have undergone.

Also there seems to be a cooling event at around 70-80 Ma in some of the sample modeling results, that is significantly younger than the Chilwa alkaline magmatism. This age seems to be quite common in the region (e.g. the Emmel et al., 2011; 2014 studies have lots of ca. 80 Ma AFT ages in Mozambique, but they don't provide an interpretation for its origin), but more work is needed to understand what caused it. We wonder if there is some undated regional magmatism or hot-fluid flow and/or mineralization of this age. A regional uplift and cooling

event at 70-80 Ma as suggested by Eby et al., (1995) is unlikely, as the cooling seems to be really fast, and it appears there was no major tectonism at this time.

Data from previous thermochronological studies from across the Malawi Rift (Van Der Beek et al., 1998; Eby et al., 1995, Mortimer et al., 2016) allows for comparison of our new data to the wider dataset and review the spread of ages across the region. Longitudinal comparison of AFT from the regional dataset clearly show relatively similar ages on the northern and southern ends of the Malawi Rift. Age against distance along rift strike seem to show a trend of younger ages near the southern fault tips, suggesting a lengthening of the fault towards the tip and a hybrid model of normal fault growth; cooling and erosion of rift flanks may be a leading cause of age variation.

The thermal and geologic history includes alkaline igneous intrusions and cooling during the Cretaceous, followed by cooling and exhumation to the surface during the Late Cretaceous to Early Cenozoic. Cenozoic East African Rift faulting and subsequent sediment deposition led to burial of the basement rocks in the various basins formed. The thermal setting of a fault zone is controlled by series of factors which include the regional geothermal structure and background thermal history of the study area, heating from friction along the wall rocks during faulting in the brittle regions and heating of the wall rocks by hot fluid flow in and around the fault zone.

5.1.1 Malombe Fault

The Malombe Fault borders the Shire Horst to the east around which the Malawi bifurcates in the southern Malawi Rift (Figure 2). The Malombe Fault incorporates 5 rock samples from the footwall scarps. The samples which included LM13, LM9, LM8B, LM7 and LM1 were all gneisses. The Cretaceous cooling ages from all the rock samples seem to represent the cooling episode associated with the Chilwa Alkaline Province that affected the region during the time period. The Malombe Fault revealed three distinct cooling episodes during

the Early Cretaceous, Late Cretaceous to Early Cenozoic and Late Cenozoic. These appear to be related to the thermal processes that accompanied the alkaline igneous intrusion in the southern Malawi Rift during the Cretaceous, post intrusion cooling, and steady minimal thermal change that preceded the East African rifting along the Malawi Rift. The third cooling episode suggests thermal activities along the faults as the Malawi rift initiates and evolves, erosion and associated uplift/exhumation.

5.1.2 Chingale-step Fault

The 2 samples (Z16 and Z22) that were collected from the Chingale-step Fault footwall scarps of the Zomba Graben are syenites and slightly foliated granite from the Chilwa Alkaline Igneous Province. The Cretaceous cooling ages estimated from the samples (Consistent with AFT cooling ages of similar samples from the region estimated by Eby et al., 1995) seem to represent the timing of the igneous intrusions in the region. AFT ages typically record post-intrusion cooling events, but if the magma is intruded into the upper crust where host rocks are resident at temperatures cooler than the PAZ, the time spent between crystallization and the first retention of fission tracks is shorter than the resolution of the dating method (Jaeger 1968). Therefore, AFT ages from shallow igneous intrusions and volcanic rocks like the ones across the Chilwa Alkaline Province can be considered as their magmatic ages. Thermochronological ages from apatite minerals that crystallized at temperatures less than the closure temperature as it often occurs in volcanic rocks and shallow intrusions, give no direct constraint on exhumation (reference). This is consistent with the thermal modelling of these samples from their mean track length distributions, exhumation is quite difficult to constrain from the samples.

5.1.3 Thyolo Fault

We collected and measured AFT cooling ages from 3 rock samples (gneisses) from the Thyolo Fault (SE17 and SE18 1-2) and its synthetic fault (Muona Fault) south-east of it (SE5-1). The samples two samples from the Thyolo Fault have Cretaceous cooling ages and that from the Muona Fault has a Cenozoic Cooling age. Thermal modelling of the samples shows three distinct cooling episodes just as the Malombe Fault and Chingale-step Fault of the southern Malawi Rift. We suggest the southern Malawi Rift and Shire Rift have experienced spatially more correlated uplift and exhumation histories throughout the Cenozoic, with the two rift systems experiencing hard and soft linkages of their border faults. This is supported by spatial trends in thermochronological data and thermal history modelling, which display similar rates of cooling across the southern Malawi Rift and the Shire Rift. The similarities in the thermal history of the faults along southern Malawi Rift (Malombe Fault and Chingale Step Fault) with the Thyolo Fault along SE of the Shire Rift indicate that these two rift systems have linked up along this axis.

5.1.4 Mwanza Fault

Three rock samples (SW2, SW7-1 and SW13) which include gneisses and a felsic dyke were collected from the fault scarps of the Mwanza Fault. These samples produced the youngest of AFT cooling ages measured from this study. Two of the samples (SW2 and SW13) have Cretaceous cooling ages and SW 13. This suggests that the Mwanza Fault has been undergoing recent thermal events and the fault itself might be of Cenozoic age even though the Shire Rift is believed to be as old as the Palaeozoic-Mesozoic. The Cretaceous age recorded by SW7 is believed to be due to the proximity of the sample to alkaline ring complexes south of the fault. The sample is believed to have recorded the cooling event associated with the alkaline igneous intrusion that occurred during the Cretaceous in the region. These intrusions are responsible for the series of dykes in the region. Due to the low fission track content of these samples, it became difficult to effectively model the thermal history of the

samples. In fact, SW2 could not provide any thermal history through modelling because of the complete lack of confined fission track lengths. Just like the samples from the Zomba Graben (Z16 and Z22), the thermal modelling does not effectively constrain the timing of exhumation. The similarities in the thermal histories of the Mwanza Fault and the Chingale-step Fault suggests that their proximities to the alkaline ring complexes that intruded during the Cretaceous makes is difficult to constraint any other thermal changes that might have occurred during the Cenozoic. The disparities between the modelled thermal history of the southern Malawi Rift and the Mwanza Fault in SW Shire Rift are believed to be due to unfavorable conditions which could include but not limited to contrasting fabric in the underlying basement, geometry and kinematics of the Mwanza Fault. The lack of linkage structures that could foster strain transfer between the two rifts along this axis (Mwanza Fault and southern Malawi Rift Faults) also supports this observation.

5.2 Fracture Pattern along the Accommodation Zone

The fracture system observed from hillshade map and slope analysis all point to the soft and hard linkages between the southern Malawi Rift and the Shire Rift. The hillshade map was used to highlight the faults and joints which are linkage structures that can foster strain transfer between the two rift systems. The density plot made from the mapped fractures (faults and joint) also show a high concentration of fractures along the accommodation zone between the southern Malawi Rift and the Shire Rift. This result suggests the presence of fracture systems capable of initiating strain transfer between the two rift systems.

The slope analysis map shows the variation of topographic slope along the border faults and also across the accommodation zone. Previous studies have investigated the relationship between relay ramps of various types (Fossen and Rotevatn, 2016, Peacock et al.,

2002). It has been established that relay ramps that have tendency to link up by a breach fault have slopes that range from 10-15^{o} at the onset of breaching (Fossen and Rotevatn, 2016). Relay ramps also demonstrate that the accommodation zone becomes steeper downwards as strain increases and becomes breached; the maximum dip of the ramp reaches around 13–14^{o} (Giba et al. 2012). This is observable in Figure 9 as the accommodation zone between the two rift systems are characterized with various fracture systems and ramp that exhibit slopes ranging from about 10-15^{o}.

The density plot generated from all the mapped fractures along the Malawi Rift and the Shire Rift also shows a high concentration of fractures in terms of length and number of fractures over a specific area with the accommodation zone between the two rift systems. This suggests recent interaction in terms of strain accommodation and transfer between the southern Malawi Rift and the Shire Rift. The density map also shows higher density of fracture at the southernmost part of the Malawi Rift which indicates that this region is undergoing Rift linkage. The zone of linkage and high fracture density also coincides with the zone described by Kolawole et al., 2021 as rift interaction zone (overlapping oblique rift interaction zones). The study by Kolawole et al., 2021 suggests that this rift interaction has recently been breached, this is consistent with the results of this study in terms of ages of tectonic uplift across the two rift systems, geometry and lack of sedimentary cover over the zone of interaction.

5.3 Strain Rates Southern Malawi Rift vs Northern Malawi Rift

The results of the strain rates calculated for this study shows a difference in the strain rates across the northern Malawi Rift compared with that of the southern Malawi rift. This result supports the hypothesis that suggests a coeval opening of the Malawi Rift with varying rate of strain accommodation from the northern segment of the rift to the

southern segment. This new data disproves the consensus of a younger southern Malawi Rift compared to the northern Malawi Rift where the rift is believed to have initiated based on the varying sedimentary fill, pattern and magnitude of strain accommodation (Specht and Rosendahl, 1989). We suggest that these disparities are due to varying rates of strain accommodation and not the ages of initiation as earlier proposed. The Malawi Rift seem to be accommodating strain faster than the southern Malawi Rift. This could be due to several reasons which include but not limited to the location of the Euler pole of rotation responsible for the movement along the two plates (Rovuma plate and Nubian Plate) rifting apart (Saria et al. 2013), the changes in lithology and rheology across the rift (see figure 1 for reference), proximity to other geologic structures (like the older Shire Rift) that can contribute to the inhibition, arrest, or termination of strain accommodation across the southern Malawi Rift (Kim and Sanderson, 2002; Bergen and Shaw, 2010).

Previous studies like Williams et al., (2021) have attempted to estimate the rate of strain accommodation along the border and intra-rift faults across the southern Malawi Rift using slip rate estimation from earthquake data. Slip rates estimated for the southern Malawi Rift from the study ranges from 0.08 to 0.5 mm/yr. Stamp et al., (2018) investigated the strain rate across the entire EARS using geodetic estimation of the motion along the moving plates. Our results for the Northern Malawi Rift seem to be consistent with their calculations for the region. Their study showed that Northern Malawi is one of the places with high strain rate magnitude which could be as high as 2 mm/yr. Stamp et al., (2008) also estimated the extension rates which is the cumulative crustal extension between the two plates rifting apart along the Malawi rift to be 2.2 mm/yr in the northern Malawi Rift and 1.5 mm/yr for the southern Malawi Rift. These previous studies (Williams et al., 2021; Stamp et al., 2021; 2018; 2008) compared to the results of our estimation of the strain rate suggests that rifting across the southern Malawi Rift might have initiated in Early Miocene (~20 - 25 Ma.) just as the

Northern Malawi Rift but larger percentage of the strain accommodation did not start accumulation until closer to the Late Miocene (~5.3 - 10 Ma.). Even though Mortimer et al., (2016) estimated the onset of rifting at 23 Ma, it was inferred from their thermal modelling of the cooling ages against mean track length plot, thermal modelling of the samples put most of their rapid cooling episodes at about ~10 Ma. Their range of onset of rapid cooling associated with rifting from thermal modelling of AFT ages (assumed from results of Van Der Beek et al., 1998) and their apatite-Helium data is from 25 Ma to less than 10 Ma. Further thermochronological studies might therefore be needed to accurately constrain the exact timing of onset of strain accommodation along the rift and subsequent tectonic episodes. Also, studies to effectively constrain the dip of the border faults and intra-rift faults is needed to reduce the uncertainty associated with the calculations of these strain rates.

5.4 Coeval Rift Model across the Malawi Rift

The debate on the model of rift growth and evolution remains a vital topic to understanding strain accommodation along plate boundaries. The results of this study from AFT thermal modelling and strain rate estimations suggests a Coeval rifting for the Cenozoic Rifting along the Malawi Rift. The age of the onset of rifting in the southern Malawi Rift compared with the estimated onset of rifting in the northern Malawi Rift (Van Der Beek et al., 1998; Mortimer et al., 2016) provide the evidence that support a coeval rifting along the Malawi Rift during the Cenozoic. The strain rates estimated for the northern and southern Malawi Rift also supports and provides explanations for the coeval model of rifting.

We propose a model that explains how strain has been accommodating across a coeval Malawi Rift since its initiation. This model of rifting illustrated in Fig. 11 shows a coeval Malawi Rift initiating as isolated faults across the entire rift during the Miocene (Figure 11a). These

isolated border faults were connected by soft linkages of series of them overlapping each other. Since the initiation of these isolated normal faults, the faults have grown by lengthening, linkage and segmentation into larger border faults and intra-rift faults by hybrid model of fault growth with alternating phases of lengthening and accrual of displacement to accommodate the cumulative strains along the faults and across the rift as manifested in the observed present-day architecture of the Malawi Rift (Fig. 11b).

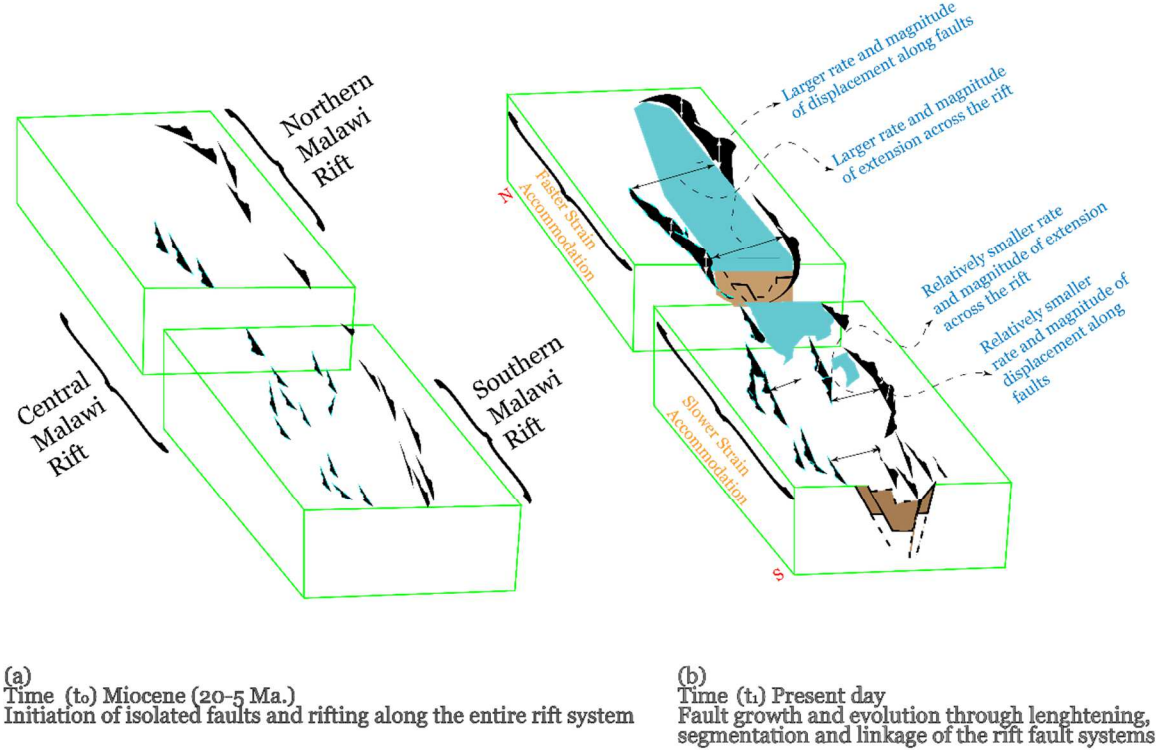

Figure 11: Conceptual Model showing the evolution of the Malawi Rift in terms of strain accommodation from initiation. (a) Coeval initiation of isolated faults across the rift segments. Some of the faults overlap by soft linkages. (b) Present-day architecture of the rift. It shows the isolated faults have coalesced by hard linkage in the north at a rate greater than the magnitude of strain accommodation in the south which have isolated faults that have grown and linked by hard linkage and more soft linkages at a slower rate compared to the northern Malawi Rift.

5.4 Implications for the history of the East African Rift

The results presented here suggest the southern Malawi Rift was initiated in the Miocene, just as the northern Malawi Rift (Fig. 11). This interpretation is contentious as active rifting across the Western Branch of the EARS is believed to have initiated in the 7–8 Ma (Ebinger, 1989; Morley and Ngenoh, 1999) and 23 Ma (Mortimer et al., 2016) which is later than in the Eastern Branch of EARS where rifting began in the Eocene (Morley and Ngenoh, 1999). Similar studies across the Eastern Branch have also highlighted cooling episodes in the Late Cretaceous–Paleocene and late Miocene–Pliocene (Foster and Gleadow, 1996; Spiegel et al., 2007). Though this corresponds to previous thermochronological studies from the Western Branch that outline the onset of cooling in thermal models in the Eocene (50 Ma–40 Ma; Van der Beek et al., 1998; Bauer et al., 2010). Stratigraphic studies and the detrital geochronology of sediment from the Rukwa Rift Basin, in the southern Western Branch, suggests active rifting began in the Oligocene (Roberts et al., 2012) and suggesting uplift of the landscape may have started even earlier and is consistent with the timing of rift initiation from thermochronological work in the Eastern Branch (Boone et al., 2019; Jess et al 2019).

The underlying mechanism that formed the EARS remains a debated topic, with both passive and active mechanisms postulated from various studies (Chorowicz, 2005). The geometry of accommodation zones could change as new rift border-fault segments and basins develop when the mechanism of rifting is changing orientations of stress during distinct episodes of rifting. As the timing of faulting and rifting in general in many parts of the Western rift system is poorly constrained, focal planes of earthquakes that are parallel to Miocene escarpments (Shudofsky, 1985) and volcanic provinces along faults aligned subparallel to border-fault systems. These have been active episodically throughout the history of their respective basins

(Ebinger, 1989; Ebinger and others, 1989). North-south propagation of rifting systems has been suggested for the Western branch of the rift system based on geomorphological evidence, just as the observed regional north-south age progression of volcanic activity recognized in the Kenya rift (Capart, 1949; Haldemann, 1969; Shackleton, 1978; Crossley and Crow, 1980; Williams and Chapman, 1986; Bosworth, 1987). Additional age constraints are needed to evaluate the trend of volcanic flows along the western branch as the volcanic intrusions from the Rungwe province (the southernmost Western rift volcanic province) are approximately 3 Ma. older than flows in the northern part of the Western rift and this contradicts the southward propagation of the Western branch (Jess et al., 2019).

Our results effectively unite the two ends of the Malawi Rift temporally and provide the means for generating a universal mechanism for the formation of the entire rift system. Though this study does not provide greater insight into a wider mechanism, it supports the notion of coeval rifting across the Malawi Rift and subsequently most parts of the western branch of EARS in the Miocene which correlates to numerous tectonic processes including rifting phases in Northern Kenya and Sudan (Bosworth, 1992; Morley et al., 1992), kinematic changes across the Indian Ocean (Cande et al., 2010) and the broader collision of African into Eurasia (Rosenbaum et al., 2002). This may suggest extension across the EARS was driven by large-scale passive tectonic processes, though active plume-related processes that initiate contemporaneous rifting must also be recognized (Jess et al., 2019; Koptev et al., 2015). Further studies of sediments within rift and rocks along the fault scarp using methods like the apatite-Helium data, which constrains cooling history at shallower depths and lower temperature annealing zone of basins across the region are necessary to further determine the timing of extensional onset. The results of this work alongside previous studies suggest coeval strain accommodation of the Western Branch of the East African Rift and thus, the modern consensus on rift initiation requires review.

CHAPTER VI

CONCLUSION

Apatite fission-track ages, history and fracture geometry from remote sensing analysis, coupled with thermal history modelling suggest the Southern Malawi Rift initiated in the Miocene and has continued to grow and evolve through multiple phases of gradual and linear uplift. We suggest the southern Malawi Rift and Shire Rift have experienced spatially more correlated uplift and exhumation histories throughout the Cenozoic, with the two rift systems experiencing hard and soft linkages of their border faults. This is supported by spatial trends in thermochronological data and thermal history modelling, which display similar rates of cooling across the southern Malawi Rift and the Shire Rift. The similarities in the thermal history of the faults along southern Malawi Rift (Malombe Fault and Chingale Step Fault) with the Thyolo Fault along SE of the Shire Rift indicate that these two rift systems have linked up along this axis. This is confirmed by the remote analyses and characterization of the fracture systems. The remote sensing analysis also shows faults and other fracture systems along the accommodation or transfer zone between the Malawi Rift and Shire Rift (Thyolo Fault) that could be responsible for strain accommodation and transfer but little to none between the Mwanza Fault and the Malawi Rift.

Even though the Shire Rift is believed to be a relic of an older rifting process that predated the East African Rift System (EARS), this study has been able to reveal that these two distinct rift systems have linked, and strain being transferred from the Malawi Rift has reactivated the Shire Rift in recent times. This study suggests that the Shire Rift has accumulated about 2 km of displacement in less than the last 5 million years. This is also consistent with the magnitude of scarp that can be observed along the Thyolo Fault.

Also, the timing of when rifting was initiated in southern Malawi Rift estimated in this study appears to be about the same range estimated by previous studies (Van Der Beek et al., 1998; Mortimer et al., 2016) for the northern Malawi Rift. This study suggests that the rifting in the northern and southern Malawi Rift probably began at about the same time but the rate of strain accumulation is responsible for the disparity in throw and displacement estimation along these sections of the Malawi Rift.

These results have broad implications for the rifting history of the Western Branch of the EAR, implying rift initiation began in the Miocene across the entire western branch and subsequent difference in the rate of strain accommodation along each rift system is responsible for the apparent southward trend of propagation along the rift system.

REFERENCES

Abbate, E., & Sagri, M. (1980). Volcanites of Ethiopian and Somali Plateaus and major tectonic lines. Atti Convegni Lincei, 47, 219-227.

Armijo, R., Tapponnier, P. & Mercier, J. 1986 Quaternary extension in southern Tibet: field observations and tectonic implications. J. Geophys. Res. 91, 13 803–13 872

Bell, R. E., Jackson, C. A.□L., Whipp, P. S., and Clements, B. (2014), Strain migration during multiphase extension: Observations from the northern North Sea, Tectonics, 33, 1936– 1963, doi:10.1002/2014TC003551.

Bonini, M., Corti, G., Innocenti, F., Manetti, P., Mazzarini, F., Abebe, T., and Pecskay, Z. (2005), Evolution of the Main Ethiopian Rift in the frame of Afar and Kenya rifts propagation, Tectonics, 24, TC1007, doi:10.1029/2004TC001680.

Brichau, S., Ring, U., Ketcham, R. A., Carter, A., Stockli, D., & Brunel, M. (2006). Constraining the long-term evolution of the slip rate for a major extensional fault system in the central Aegean, Greece, using thermochronology. Earth and Planetary Science Letters, 241(1-2), 293-306.

Brun, J.-P. & Choukroune, P. (1983). Normal faulting, block tilting and decollement in a stretched crust. Tectonics 2, 345–356.

Brune, S., Corti, G., and Ranalli, G. (2017), Controls of inherited lithospheric heterogeneity on rift linkage: Numerical and analog models of interaction between the Kenyan and Ethiopian rifts across the Turkana depression, Tectonics, 36, 1767– 1786, doi:10.1002/2017TC004739.

Buck, R. W. (1991) Modes of continental lithospheric extension. J. Geophys. Res. 96, 20 161– 20 178.

Calais, E., d'Oreye, N., Albaric, J. et al. (2008). Strain accommodation by slow slip and dyking in a youthful continental rift, East Africa. Nature 456, 783–787 https://doi.org/10.1038/nature07478

Carrapa, B., (2010), Resolving tectonic problems by dating detrital minerals: Geology, v. 38, p. 191–192.

Carrapa, B., S. Bywater-Reyes, P. G. DeCelles, E. Mortimer, and G. E. Gehrels, (2011), Late Eocene–Pliocene basin evolution in the Eastern Cordillera of northwestern Argentina (25°–26°S): regional implications for Andean orogenic wedge development: *Basin Research*.

Carter, A., & Gallagher, K. (2004). Characterizing the significance of provenance on the inference of thermal history models from apatite fission-track data-a synthetic data study. *Special Papers-Geological Society of America*, 7-24.

Carter, A., & Foster, G. L. (2006). Enhanced source characterisation through combined FT and Sm–Nd on single detrital apatites. *Geochimica et Cosmochimica Acta*, *18*(70), A86.

Castaing, C. (1991). Post-Pan-African tectonic evolution of South Malawi in relation to the Karroo and recent East African rift systems. *Tectonophysics, 191(1–2)*, 55–73. https://doi.org/10.1016/0040-1951(91)90232-H

Coney, P. J. & Harms, T. A. (1984) Cordilleran metamorphic core complexes: Cenozoic extensional relics of Mesozoic compression. Geology 12, 550–554.

Corti, G. (2009). Continental rift evolution: from rift initiation to incipient break-up in the Main Ethiopian Rift, East Africa. *Earth-science reviews*, *96*(1-2), 1-53.

Cowie, P. A., Underhill, J. R., Behn, M. D., Lin, J., & Gill, C. E. (2005). Spatio-temporal evolution of strain accumulation derived from multi-scale observations of Late Jurassic rifting in the northern North Sea: A critical test of models for lithospheric extension. *Earth and Planetary Science Letters*, *234*(3-4), 401-419.

Craig, T.J., Jackson, J.A., Priestley, K., and Mckenzie, D., (2011), Earthquake distribution patterns in Africa: Their relationship to variations in lithospheric and geological structure, and their

rheological implications: Geophysical Journal International, v. 185, p. 403–434, https://doi.org/10.1111/j.1365-246X.2011.04950.x.

Daszinnies, Matthias & Emmel, Benjamin & Jacobs, Joachim & Grantham, Geoff & Thomas, Bob. (2008). Denudation In Southern Malawi and Northern Mozambique: Indications of the Long-term Tectonic Segmentation of East Africa During the Gondwana Break-up.

Daszinnies, M.C., Jacobs, J., Wartho, J.A., and Grantham, G.H., 2009, Post Pan-African thermo-tectonic evolution of the north Mozambican basement and its implication for the Gondwana rifting. Inferences from 40Ar/39Ar hornblende, biotite and titanite fission-track dating: Geological Society, London, Special Publications, v. 324, p. 261–286, doi:10.1144/SP324.18.

Deeken, A., E. R. Sobel, I. Coutand, M. Haschke, U. Riller, and M. R. Strecker, (2006), Development of the southern Eastern Cordillera, NW Argentina, constrained by apatite fission track thermochronology: from early Cretaceous extension to middle Miocene shortening: *Tectonics, v. 25*.

Deng, H., Ren, J., Pang, X., Rey, P. F., McClay, K. R., Watkinson, I. M., ... & Luo, P. (2020). South China Sea documents the transition from wide continental rift to continental break up. *Nature Communications*, *11*(1), 1-9. https://doi.org/10.1038/s41467-020-18448-y

Ebinger, C. J., Deino, A. L., Drake, R. E., & Tesha, A. L. (1989). Chronology of volcanism and rift basin propagation: Rungwe volcanic province, East Africa. *Journal of Geophysical Research, 94(B11)*. https://doi.org/10.1029/jb094ib11p15785

Ebinger, C. (2005). Continental break-up: the East African perspective. *Astronomy & Geophysics*, *46*(2), 2-16.

Ebinger, C., & Scholz, C. A. (2011). Continental rift basins: the East African perspective. *Tectonics of sedimentary basins: Recent advances*, 183-208.

Ebinger, C.J., Oliva, S.J., Pham, T-Q., Peterson, K., Chindandali, P., Illsley-Kemp, F., Drooff, C.,

Eby, G. N., Roden-Tice, M., Krueger, H. L., Ewing, W., Faxon, E. H., & Woolley, A. R. (1995). Geochronology and cooling history of the northern part of the Chilwa Alkaline Province, Malawi. Journal of African Earth Sciences, 20(3–4), 275–288. https://doi.org/10.1016/0899-5362(95)00054-W

Emmel, B., Kumar, R., Ueda, K., Jacobs, J., Daszinnies, M.C., Thomas, R.J., and Matola, R., 2011, Thermochronological history of an orogen-passive margin system: An example from northern Mozambique: Tectonics, v. 30, p. TC2002, doi:10.1029/2010TC002714.

Emmel, B., Kumar, R., Jacobs, J., Ueda, K., Van Zuilen, M., and Matola, R., 2014, The low-temperature thermochronological record of sedimentary rocks from the central Rovuma Basin (N Mozambique) — Constraints on provenance and thermal history: Gondwana Research, v. 25, p. 1216–1229, doi:10.1016/j.gr.2013.05.008.

England, P., and Molnar, P., 1990, Surface Uplift, Uplift of Rocks, and Exhumation of Rocks: Geology, v. 18, p. 1173–1177.

Faulds, J. E., & Varga, R. J. (1998). The role of accommodation zones and transfer zones in the regional segmentation of extended terranes. *Geological Society of America Special Papers*, *323*, 1-45.

Flannery, J. W., & Rosendahl, B. R. (1990). The seismic stratigraphy of Lake Malawi, Africa: implications for interpreting geological processes in lacustrine rifts. *Journal of African Earth Sciences, 10(3)*, 519–548. https://doi.org/10.1016/0899-5362(90)90104-M

Fitzgerald, P. G., Duebendorfer, E. M., Faulds, J. E., & O'Sullivan, P. (2009). South Virgin–White Hills detachment fault system of SE Nevada and NW Arizona: Applying apatite fission track thermochronology to constrain the tectonic evolution of a major continental detachment fault. *Tectonics*, *28*(2).

Foster, A.N., and Jackson, J.A., (1998), Source parameters of large African earthquakes: Implications for crustal rheology and regional kinematics: Geophysical Journal International, https://doi.org/10.1046/j.1365-246x.1998.00568.x.

Furman, T., Bryce, J. G., Karson, J., & Iotti, A. (2004). East African Rift System (EARS) plume structure: insights from Quaternary mafic lavas of Turkana, Kenya. *Journal of Petrology*, *45*(5), 1069-1088.

Gallagher, K., Hawkesworth, C. J., & Mantovani, M. S. M. (1995). Denudation, fission track analysis and the long-term evolution of passive margin topography: application to the southeast Brazilian margin. *Journal of South American Earth Sciences, 8(1)*, 65-77.

Gallagher, K., and Brown, R., 1997, The onshore record of passive margin evolution: Journal of The Geological Society, v. 154, p. 451–457.

Gallagher, K., Brown, R.W., and Johnson, C., 1998, Fission Track Analysis and its Application to Geological Problems: Annual Reviews in Earth and Planetary Sciences, v. 26, p. 519–572.

Gleadow, A.J.W., Duddy, I.R., Green, P.F., and Lovering, J.F., 1986, Confined fission track lengths in apatite: a diagnostic tool for thermal history analysis: Contributions to Mineralogy and Petrology, v. 94, p. 405–415.

Goldsworthy, M., & Jackson, J. (2001). Migration of activity within normal fault systems: examples from the Quaternary of mainland Greece. *Journal of Structural Geology*, *23*(2-3), 489-506.

Green, P.F., 1986, On the Thermo-Tectonic Evolution of Northern England - Evidence from Fission-Track Analysis: Geological Magazine, v. 123, p. 493–506.

Hey, R. (1977). A new class of "pseudofaults" and their bearing on plate tectonics: A propagating rift model. Earth and Planetary Science Letters, 37(2), 321-325.

Ketcham, R.A., Carter, A., Donelick, R.A., Barbarand, J., and Hurford, A.J., 2007, Improved modeling of fission-track annealing in apatite: American Mineralogist, v. 92, p. 799–810, doi:10.2138/am.2007.2281.

Kim, Y. S., Peacock, D. C., & Sanderson, D. J. (2004). Fault damage zones. Journal of structural geology, 26(3), 503-517.

Kolawole, F., Firkins, M. C., Al Wahaibi, T. S., Atekwana, E. A., & Soreghan, M. J. (2021). Rift Transfer Zones and the Stages of Rift Linkage in Active Segmented Continental Rift Systems.

Laó-Dávila, D. A., Al-Salmi, H. S., Abdelsalam, M. G., & Atekwana, E. A. (2015). Hierarchical segmentation of the Malawi Rift: The influence of inherited lithospheric heterogeneity and kinematics in the evolution of continental rifts. *Tectonics, 34(12)*, 2399–2417. https://doi.org/10.1002/2015TC003953

Lavier, L. L., & Manatschal, G. (2006). A mechanism to thin the continental lithosphere at magma-poor margins. *Nature*, *440*(7082), 324-328.

Lutz, T.M., and Omar, G.I., (1991), Inverse methods of modeling thermal histories from apatite fission-track data, *Earth Planet. Sci. Lett., v. 104*, p. 181-195

Macgregor, D., (2015), History of the development of the East African Rift System: A series of interpreted maps through time: Journal of African Earth Sciences, v. 101, p. 232–252, https://doi.org/10.1016/j.jafrearsci.2014.09.016.

Mahatsente, R., Jentzsch, G., & Jahr, T. (1999). Crustal structure of the Main Ethiopian Rift from gravity data: 3-dimensional modeling. *Tectonophysics*, *313*(4), 363-382.

Maguire, P. K. H., Ebinger, C. J., Stuart, G. W., Mackenzie, G. D., Whaler, K. A., Kendall, J. M., ... & Harder, S. (2003). Geophysical project in Ethiopia studies continental breakup. *EOS, Transactions American Geophysical Union*, *84*(35), 337-343.

Morley, C. K., Nelson, R. A., Patton, T. L., & Munn, S. G. (1990). Transfer zones in the East African rift system and their relevance to hydrocarbon exploration in rifts. *AAPG bulletin*, *74*(8), 1234-1253.

Morley, C. K. (1999). Patterns of displacement along large normal faults: implications for basin evolution and fault propagation, based on examples from East Africa. *AAPG bulletin*, *83*(4), 613-634.

Mortimer, E., Kirstein, L. A., Stuart, F. M., & Strecker, M. R. (2016). Spatio-temporal trends in normal-fault segmentation recorded by low-temperature thermochronology: Livingstone fault scarp, Malawi Rift, East African Rift System. *Earth and Planetary Science Letters, 455*, p. 62–72. https://doi.org/10.1016/j.epsl.2016.08.040

Muirhead, J. D., Kattenhorn, S. A., Lee, H., Mana, S., Turrin, B. D., Fischer, T. P., ... & Stamps, D. S. (2016). Evolution of upper crustal faulting assisted by magmatic volatile release during early-stage continental rift development in the East African Rift. *Geosphere*, *12*(6), 1670-1700.

Muirhead, J. D., Wright, L. J., & Scholz, C. A. (2019). Rift evolution in regions of low magma input in East Africa. *Earth and Planetary Science Letters*, *506*, 332-346.

Nixon, C. W., McNeill, L. C., Bull, J. M., Bell, R. E., Gawthorpe, R. L., Henstock, T. J., ... & Ferentinos, G. (2016). Rapid spatiotemporal variations in rift structure during development of the Corinth Rift, central Greece. *Tectonics*, *35*(5), 1225-1248.

Péron-Pinvidic, G., & Manatschal, G. (2009). The final rifting evolution at deep magma-poor passive margins from Iberia-Newfoundland: a new point of view. *International Journal of Earth Sciences*, *98*(7), 1581-1597.

Peyton S. L., Carrapa B., (2013), An introduction to low-temperature thermochronologic techniques, methodology, and applications, *in* C. Knight and J. Cuzella, eds., Application of structural methods to Rocky Mountain hydrocarbon exploration and development: *AAPG Studies in Geology 65*, p. 15–36.

Raab, M. J., Brown, R. W., Gallagher, K., Weber, K., & Gleadow, A. J. W. (2005). Denudational and thermal history of the Early Cretaceous Brandberg and Okenyenya igneous complexes on Namibia's Atlantic passive margin. *Tectonics, 24(3),* https://doi.org/10.1029/2004TC001688

Raab, Matthias J., Brown, R. W., Gallagher, K., Carter, A., & Weber, K. (2002). Late Cretaceous reactivation of major crustal shear zones in northern Namibia: Constraints from apatite fission track analysis. *Tectonophysics, 349(1–4),* 75–92. https://doi.org/10.1016/S0040-1951(02)00047-1

Reiners, P.W., Ehlers, T.A., and Zeitler, P.K., 2005, Past, present, and future of thermochronology: Reviews in Mineralogy and Geochemistry, v. 58, p. 1–18, doi:10.2138/rmg.2005.58.1.

Ring, U., Betzler, C., & Delvaux, D. (1992). Normal vs. strike-slip faulting during rift development in East Africa: the Malawi rift. *Geology, 20(11)*, 1015-1018.

Rosendahl, B. R. (1987). Architecture of continental rifts with special reference to East Africa. *Annual Review of Earth and Planetary Sciences*, *15*, 445.

Saria, E., Calais, E., Altamimi, Z., Willis, P., & Farah, H. (2013). A new velocity field for Africa from combined GPS and DORIS space geodetic solutions: contribution to the definition of the African reference frame (AFREF). Journal of Geophysical Research: Solid Earth, 118(4), 1677-1697.

Scholz, C. H., & Contreras, J. C. (1998). Mechanics of continental rift architecture. *Geology*, *26*(11), 967-970.

Shillington, D.J., Accardo, N.J., Gallacher, R.J., Gaherty, J., Nyblade, A.A., and Mulibo, G., (2019), Kinematics of Active Deformation in the Malawi Rift and Rungwe Volcanic Province, Africa: Geochemistry, Geophysics, Geosystems, v. 20, p. 3928–3951, https://doi.org/10.1029/2019GC008354.

Specht, T. D., & Rosendahl, B. R. (1989). Architecture of the Lake Malawi Rift, East Africa. *Journal of African Earth Sciences, 8(2–4)*, 355–382. https://doi.org/10.1016/S0899-5362(89)80032-6

Stamps, D. S., Calais, E., Saria, E., Hartnady, C., Nocquet, J. M., Ebinger, C. J., & Fernandes, R. M. (2008). A kinematic model for the East African Rift. Geophysical Research Letters, 35(5).

Stamps, D. S., Saria, E., & Kreemer, C. (2018). A geodetic strain rate model for the East African Rift System. Scientific reports, 8(1), 1-9.

Stamps, D. S., Kreemer, C., Fernandes, R., Rajaonarison, T. A., & Rambolamanana, G. (2021). Redefining East African Rift System kinematics. Geology, 49(2), 150-155.

Stockli D. F. (2005). Application of Low-Temperature Thermochronometry to Extensional Tectonic Settings. *Reviews in Mineralogy and Geochemistry; 58 (1)*: 411–448. doi: https://doi.org/10.2138/rmg.2005.58.16

Thomson, S. N., Stöckhert, B., & Brix, M. R. (1998). Thermochronology of the high-pressure metamorphic rocks of Crete, Greece: Implications for the speed of tectonic processes. *Geology, 26(3)*, 259–262. https://doi.org/10.1130/0091-7613(1998)026<0259:TOTHPM>2.3.CO;2

Van der Beek, P., Mbede, E., Andriessen, P., & Delvaux, D. (1998). Denudation history of the Malawi and Rukwa Rift flanks (East African Rift system) from apatite fission track thermochronology. *Journal of African Earth Sciences, 26(3)*, 363–385. https://doi.org/10.1016/S0899-5362(98)00021-9

Wedmore, L. N., Biggs, J., Williams, J. N., Fagereng, Å., Dulanya, Z., Mphepo, F., & Mdala, H. (2020). Active fault scarps in southern Malawi and their implications for the distribution of strain in incipient continental rifts. *Tectonics*, *39*(3), e2019TC005834.

Woldegabriel, G., Aronson, J. L., & Walter, R. C. (1990). Geology, geochronology, and rift basin development in the central sector of the Main Ethiopia Rift. *Geological Society of America Bulletin*, *102*(4), 439-458.

WoldeGabriel, G., Olago, D., Dindi, E., & Owor, M. (2016). Genesis of the east African rift system. In *Soda Lakes of East Africa* (pp. 25-59). Springer, Cham.

Zanettin, B., EJ, V., & EM, P. (1979). Correlation Among Ethiopian Volcanic Formation with Special Reference to the Chronological and Stratigraphical Problems of the Trap Series.

VITA

Oyewande Olumide Ojo

Candidate for the Degree of

Master of Science

Thesis: ONSET OF THE NEOGENE - QUATERNARY CONTINENTAL SOUTHERN MALAWI RIFT AND LINKAGE TO THE LATE CARBONIFEROUS – EARLY JURASSIC SHIRE RIFT

Major Field: Geology

Biographical:

Education:
Completed the requirements for the Master of Science in Geology at Oklahoma State University, Stillwater, Oklahoma in July, 2021.

Completed the requirements for the Bachelor of Science in Geology at University of Ibadan, Ibadan, Nigeria in 2015.

Experience:
Teaching Assistant. 2019-Present. Boone Pickens School of Geology, Oklahoma State University

Subject Teacher. 2016-2017. Ayila Senior High School, Ayila, Nigeria

Field Geologist (Industrial Trainee). 2015. Safeway Drilling, Ibadan, Nigeria

Professional Memberships:
Nigerian Association of Petroleum Explorationists (NAPE)

American Association of Petroleum Geology (AAPG)

Geological Society of America (GSA)

American Institute of Professional Geologist

American Geophysical Union (AGU)